SUPPLEMENTAL DATA

Table S1. Related to Figure 1. Pre-BCR and BCL6 expression and function of patient-derived ALL samples and cell lines studied

Case	Lesion	pre-BCR expression	pre-BCR function	BCL6 expression	STAT5-activity
ICN12	*TCF3-PBX1*	μHC, λ5, VpreB	Src, Syk, Btk, Ca^{2+}	BCL6	negative
JFK3	*PBX1,* del6q21	μHC, λ5, VpreB	n.d.	BCL6	negative
JFK4	*TCF3-PBX1*	μHC, λ5	n.d.	BCL6	negative
JFK5	*TCF3-PBX1*	μHC, λ5	n.d.	BCL6	negative
JFK6	*TCF3-PBX1*	μHC, λ5	n.d.	BCL6	negative
JFK7	*TCF3-PBX1*	μHC, λ5	n.d.	BCL6	negative
PDX60 (11064)	*TCF3-PBX1*	μHC, λ5, VpreB	Src, Syk, Btk	BCL6	negative
PDX61 (7112)	*TCF3-PBX1*	μHC, λ5, VpreB	Src, Syk, Btk	BCL6	negative
SFO7	*TCF3-PBX1*	μHC, λ5, VpreB	n.d.	BCL6	negative
SFO8	*TCF3-PBX1*	μHC, λ5, VpreB	n.d.	BCL6	negative
PDX62 (09-565)	Hypodiploid	μHC, λ5, VpreB	n.d.	BCL6	negative
ICN6	*ETV6-RUNX1*	negative	negative	negative	STAT5-pY^{694}
ICN3	*MLL-AF4*	negative	negative	negative	negative
ICN13	*MLL-AF4*	negative	negative	negative	STAT5-pY^{694}
ICN1	*BCR-ABL1*	negative	negative	negative	STAT5-pY^{694}
BLQ1	*BCR-ABL1*	negative	negative	negative	STAT5-pY^{694}
BLQ5	*BCR-ABL1*	negative	negative	negative	STAT5-pY^{694}
LAX2	*BCR-ABL1*	negative	negative	negative	STAT5-pY^{694}
LAX9	*BCR-ABL1*	negative	negative	negative	STAT5-pY^{694}
BLQ6	*BCR-ABL1*	negative	n.d.	negative	STAT5-pY^{694}
SFO2	*BCR-ABL1*	negative	negative	negative	STAT5-pY^{694}
PDX2	*BCR-ABL1*	negative	negative	negative	STAT5-pY^{694}
PDX14	*BCR-ABL1*	negative	n.d.	negative	STAT5-pY^{694}
TXL2	*BCR-ABL1*	negative	n.d.	negative	STAT5-pY^{694}
MXP2	*BCR-ABL1*	negative	negative	negative	STAT5-pY^{694}
MXP3	*BCR-ABL1*	negative	negative	negative	STAT5-pY^{694}
LAX7	unknown	negative	negative	negative	STAT5-pY^{694}
LAX7R	*KRAS*^{G12C}	negative	negative	negative	negative
SFO3	unknown	negative	negative	negative	STAT5-pY^{694}
SFO5	unknwon	negative	negative	negative	STAT5-pY^{694}
PDX15	*GNB1*^{K89I}	negative	negative	negative	STAT5-pY^{694}

Cell line	Lesion	pre-BCR expression	pre-BCR function	BCL6 expression	STAT5-activity
SMS-SB	*PDGFR*	μHC, λ5, VpreB	Src, Syk, Btk	BCL6	negative
697	*TCF3-PBX1*	μHC, λ5, VpreB	Src, Syk, Btk, Ca^{2+}	BCL6	negative
Kasumi-2	*TCF3-PBX1*	μHC, λ5, VpreB	Src, Syk, Btk, Ca^{2+}	BCL6	negative
RCH-ACV	*TCF3-PBX1*	μHC, λ5, VpreB	Src, Syk, Btk, Ca^{2+}	BCL6	negative
MHH-CALL3	*TCF3-PBX1*	λ5, VpreB	Ca^{2+}	BCL6	negative
Nalm6	*ETV6-PDGFRB*	μHC, λ5, VpreB	Src, Syk, Btk, Ca^{2+}	BCL6	negative
HPB-NULL	del(6)(q21)	μHC, λ5, VpreB	Src, Syk, Btk, Ca^{2+}	BCL6	negative
BV173	*BCR-ABL1*	negative	negative	negative	STAT5-pY^{694}
Nalm1	*BCR-ABL1*	negative	negative	negative	STAT5-pY^{694}
SUP-B15	*BCR-ABL1*	negative	negative	negative	STAT5-pY^{694}
Tom1	*BCR-ABL1*	negative	negative	negative	STAT5-pY^{694}
BEL1	*MLL-AF4*	negative	negative	n.d.	STAT5-pY^{694}
RS4;11	*MLL-AF4*	negative	negative	n.d.	STAT5-pY^{694}
SEM	*MLL-AF4*	negative	negative	n.d.	STAT5-pY^{694}
REH	*ETV6-RUNX1*	negative	negative	negative	STAT5-pY^{694}

Note: All primary samples are bone marrow biopsies, blast content >80%; LAX, Los Angeles, CA; BLQ, Bologna IT; TXL, Berlin, DE; SFO, San Francisco, CA; ICN, Seoul, KR; PDX, Portland, OR; MXP, Milan, IT; JFK, New York, NY; n.d. not done. BCL6 expression and STAT5-activity were measured by Western blot using antibodies against BCL6 and phospho-STAT5-pY^{694}.

Table S2. Related to Figure 1. Overview of patient-derived ALL samples studied

Case	Cytogenetics	Oncogene	Clinical course	Gender/Age
ICN12	t(1;19)(q23;p13)	*TCF3-PBX1*	at diagnosis	f/8
JFK3	46,XX[13]/46,XX, der(19)t(1;19) (q23;p13)	*TCF3-PBX1*	at diagnosis	m/46
JFK4	44-45,XY,-7,der(9)t(7;9)(q11.2;p21),	*TCF3-PBX1*	at diagnosis	m/35
JFK5	46,XY,der(19)t(1;19)(q23;p13)[16]/46,XY[4]	*TCF3-PBX1*	at diagnosis	m/20
JFK6	46,XX[13]/46,XX,i(9)(q10), der(19)t(1;19) (q23;p13)	*TCF3-PBX1*	at diagnosis	f/60
JFK7	46,XX,t(9;11)(p24;q14)?c[2]/47~49,idem,-2,	*TCF3-PBX1*	at diagnosis	f/55
PDX60	46,XY,der(19)t(1;19)(q23;p13.3) del(6)(q21)	*TCF3-PBX1*		m
PDX61	44-45,XY,-7,der(9)t(7;9)(q11.2;p21),add(19)	*TCF3-PBX1*		m
SFO7	46,XX,del(13)(q12q14),der(19)t(1;19)(q23;p13)	*TCF3-PBX1*	at diagnosis	f/9
SFO8	47,XY,+8,t(14;19)(q32;q13.1),der(19)t(1;19)	*TCF3-PBX1*	at diagnosis	m/27
PDX62	<44 Chromosomes		at diagnosis	
ICN6	t(12;21)(p13;q22)	*ETV6-RUNX1*	at diagnosis	m/3
ICN3	t(4;11)(q21;q23)	*MLL-AF4*		m/5
ICN13	t(4;11)(q21;q23)	*MLL-AF4*		f/15
ICN1	t(9;22)(q34;q11)	*BCR-ABL1*; p210,	at diagnosis	
BLQ1	FISH der(9), der(22)	*BCR-ABL1*; p210, T315I	Relapse (Imatinib)	
BLQ5	FISH der(9), der(22)	*BCR-ABL1*; p190, T315I	Relapse (Imatinib)	f
LAX2	t(9;22)(q34;q11)	*BCR-ABL1*; p210, T315I	Relapse (Imatinib)	m/38
LAX9	t(9;22)(q34;q11), del(12)(p12;p13); del(11)(q23)	*BCR-ABL1*; p190,	at diagnosis m	
BLQ6	t(9;22)(q34;q11)	*BCR-ABL1*; p210, T315I	Relapse (Imatinib)	m
SFO2	t(9;22)(q34;q11)	*BCR-ABL1*; p210,	at diagnosis	m/7
PDX2		*BCR-ABL1*	at diagnosis	f/52
PDX14	45~46,XY,del(9)(p?21), t(9;22)(q34;q11.2)	*BCR-ABL1*	at diagnosis	m/36
TXL2	t(9;22)(q34;q11)	*BCR-ABL1*	at diagnosis	m/63
MXP2	t(9;22)(q34;q11)	*BCR-ABL1*; p190		/6
MXP3	t(9;22)(q34;q11)	*BCR-ABL1*; p190		/13
LAX7			at diagnosis	
LAX7R		$KRAS^{G12V}$	Relapse	
SFO3			Relapse	
SFO5				
PDX15			at diagnosis	f/29

Note: All primary samples are bone marrow biopsies, blast content >80%; LAX, Los Angeles, CA; BLQ, Bologna IT; TXL, Berlin, DE; SFO, San Francisco, CA; ICN, Seoul, KR; PDX, Portland, OR; MXP, Milan, IT; JFK, New York, NY; f, female; m, male

Table S3. Related to Figure 1. Overview of ALL cell lines studied

Cell line	Genetic Lesion	Gender/Age	Source
SMS-SB	*PDGFR*	f/16	Dr. Jan A. Burger, MDACC
697	*TCF3-PBX1*	m/12	DSMZ
Kasumi-2	*TCF3-PBX1*	m/15	DSMZ
RCH-ACV	*TCF3-PBX1*	f/8	DSMZ
MHH-CALL3	*TCF3-PBX1*	f/11	DSMZ
Nalm6	*ETV6-PDGFRB*	m/19	DSMZ
HPB-NULL	del(6)(q21)	m/47	Dr. Hassan Jumaa, Freiburg
BV173	*BCR-ABL1*		DSMZ
Nalm1	*BCR-ABL1*	f/3	DSMZ
SUP-B15	*BCR-ABL1*	m/9	DSMZ
Tom1	*BCR-ABL1*	f/54	DSMZ
BEL1	*MLL-AF4*	f/41	Dr. Ruoping Tang, Paris, France
RS4;11	*MLL-AF4*	f/32	DSMZ
SEM	*MLL-AF4*	f/5	DSMZ
REH	*ETV6-RUNX1*	f/15	DSMZ

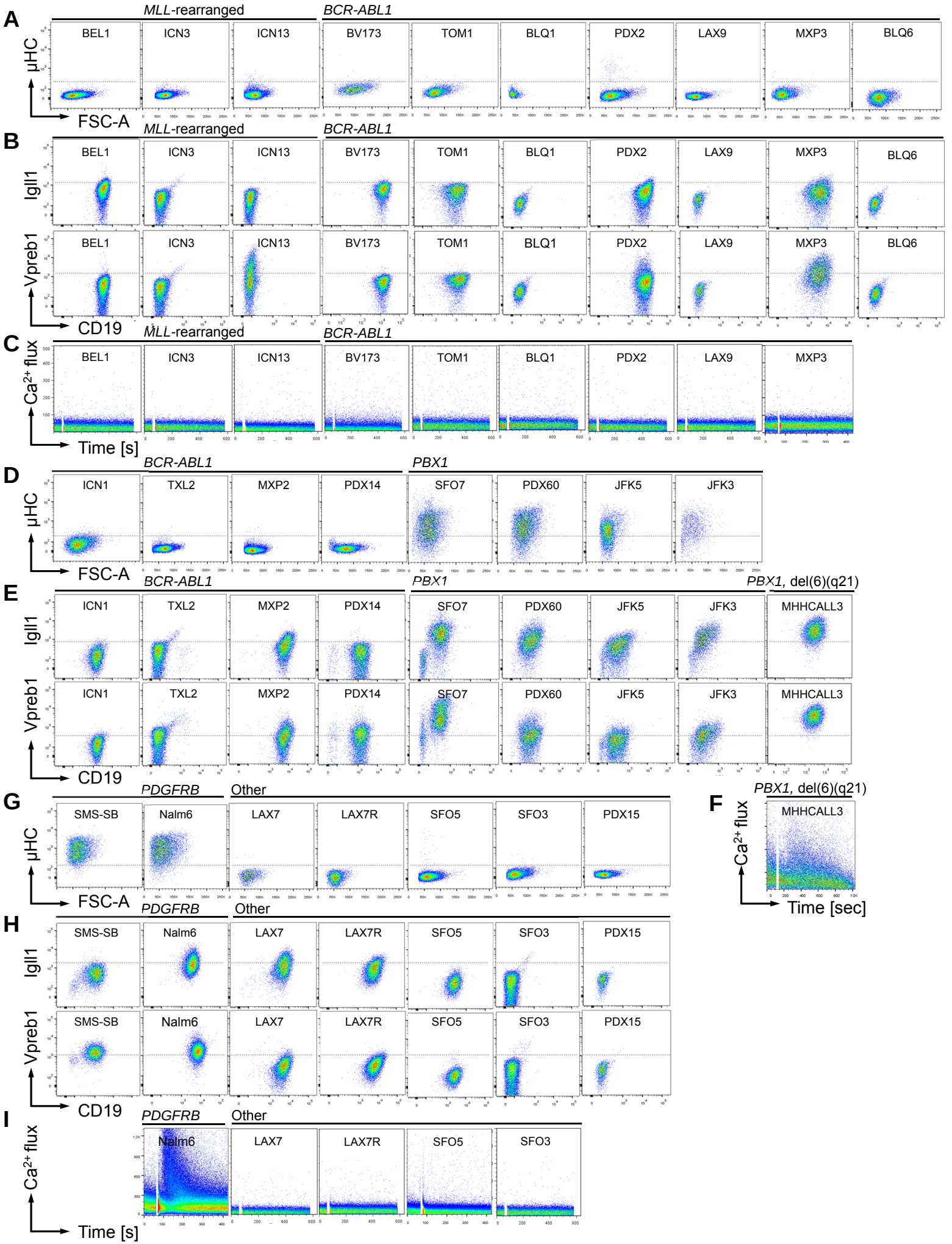
A
MLL-rearranged
BCR-ABL1
BEL1
ICN3
ICN13
BV173
TOM1
BLQ1
PDX2
LAX9
MXP3
BLQ6
μHC
FSC-A
B
MLL-rearranged
BCR-ABL1
Igll1
Vpreb1
CD19
C
MLL-rearranged
BCR-ABL1
Ca2+ flux
Time [s]
D
BCR-ABL1
PBX1
ICN1
TXL2
MXP2
PDX14
SFO7
PDX60
JFK5
JFK3
E
BCR-ABL1
PBX1
PBX1, del(6)(q21)
MHHCALL3
F
PBX1, del(6)(q21)
MHHCALL3
Time [sec]
G
PDGFRB
Other
SMS-SB
Nalm6
LAX7
LAX7R
SFO5
SFO3
PDX15
H
I

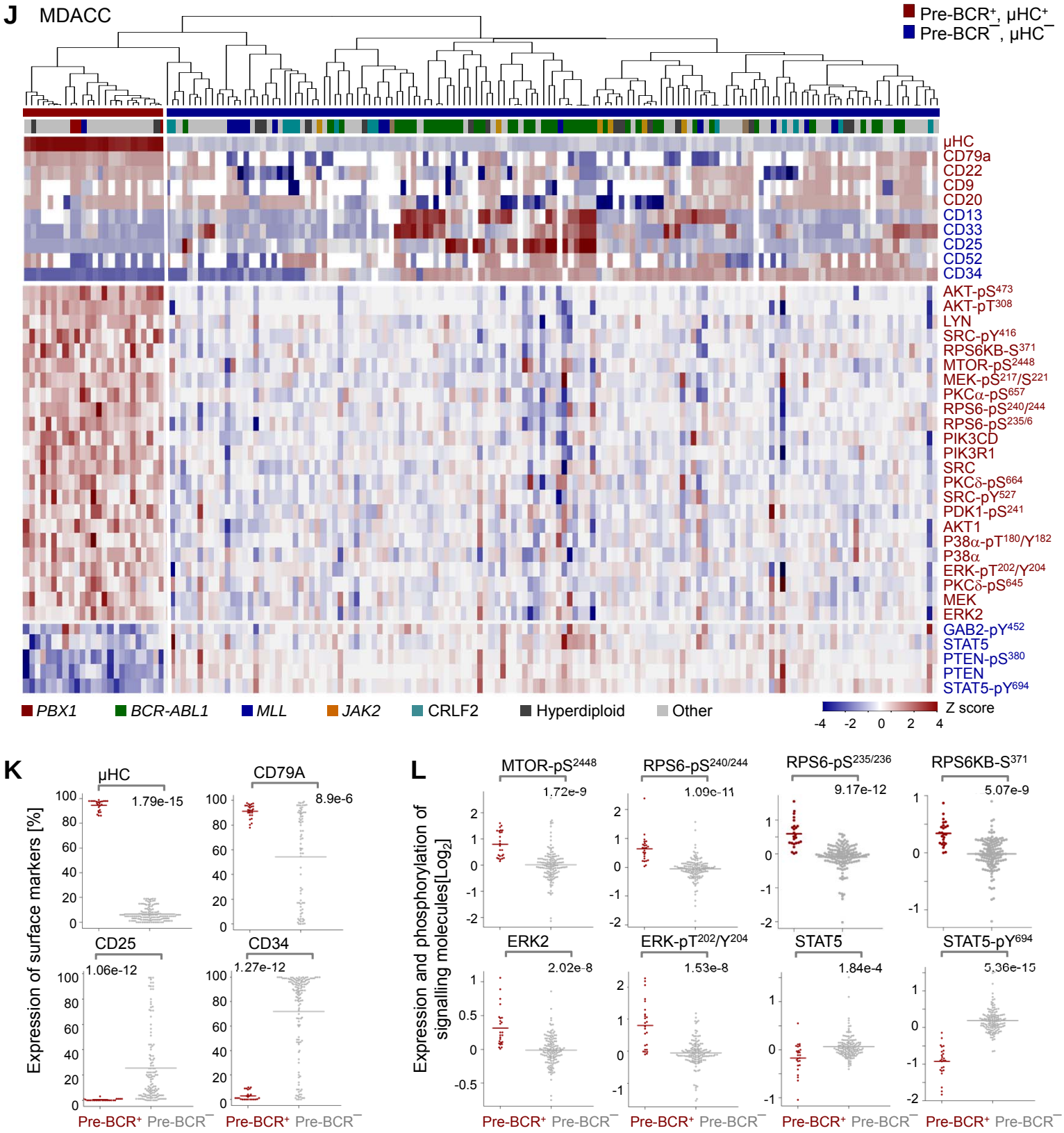
J
MDACC
Pre-BCR+, μHC+
Pre-BCR−, μHC−
μHC
CD79a
CD22
CD9
CD20
CD13
CD33
CD25
CD52
CD34
AKT-pS473
AKT-pT308
LYN
SRC-pY416
RPS6KB-S371
MTOR-pS2448
MEK-pS217/S221
PKCα-pS657
RPS6-pS240/244
RPS6-pS235/6
PIK3CD
PIK3R1
SRC
PKCδ-pS664
SRC-pY527
PDK1-pS241
AKT1
P38α-pT180/Y182
P38α
ERK-pT202/Y204
PKCδ-pS645
MEK
ERK2
GAB2-pY452
STAT5
PTEN-pS380
PTEN
STAT5-pY694
PBX1
BCR-ABL1
MLL
JAK2
CRLF2
Hyperdiploid
Other
Z score
-4 -2 0 2 4
K
μHC
1.79e-15
CD79A
8.9e-6
CD25
1.06e-12
CD34
1.27e-12
Expression of surface markers [%]
Pre-BCR+ Pre-BCR−
Pre-BCR+ Pre-BCR−
L
MTOR-pS2448
1.72e-9
RPS6-pS240/244
1.09e-11
RPS6-pS235/236
9.17e-12
RPS6KB-S371
5.07e-9
ERK2
2.02e-8
ERK-pT202/Y204
1.53e-8
STAT5
1.84e-4
STAT5-pY694
5.36e-15
Expression and phosphorylation of signalling molecules[Log2]
Pre-BCR+ Pre-BCR−
Pre-BCR+ Pre-BCR−
Pre-BCR+ Pre-BCR−
Pre-BCR+ Pre-BCR−

Figure S1. Related to Figure 1. Expression and activity of the pre-B cell receptor in subsets of pre-B ALL. (**A,D,G**) Flow cytometry staining for cytoplasmic μHC. (**B,E,H**) Flow cytometry staining for surface expression of the surrogate light chain components λ5 (Igll1) and Vpreb1. (**C,F,I**) Flow cytometry staining for Ca^{2+} mobilization in response to pre-BCR engagement using μHC-specific antibodies, were studied in a series of pre-B ALL cell lines and patient-derived samples. (**J**) Expression of immunophenotypic markers were measured by flow cytometry (*top* panel) and expression and phosphorylation of 66 signaling molecules were measured by reverse phase protein arrays (RPPA, *bottom* panel) on pre-B ALL patient samples from M.D. Anderson Medical Center (MDACC 1983-2007; n=208). Patient samples were divided into pre-BCR^+ and pre-BCR^- groups based on flow cytometry measurements of pre-BCR (μHC) and the Igα signaling chain CD79A expression. The clustering dendrogram showed that pre-BCR^+ cases were clustered together based on the expression of the immunophenotypic markers. Supervised analysis on pre-BCR^+ vs. pre-BCR^- ALL cases showed differential expression of the signalling molecules. (**K**) Expression on μHC (cytoplasmic), CD79A, CD25 and CD34 by flow cytometry, and (**L**) expression on p-MTOR, p-RPS6, p-RPS6KB, ERK, p-ERK, STAT5 and p-STAT5 by RPPA, were shown in pre-BCR^+ and pre-BCR^- ALL groups. P values were calculated by two-sided Wilcoxon test.

Table S4. Related to Figure 2. *IGHM* gene rearrangements in human pre-B ALL

V_H-DJ_H junctions in human normal B cell precursors (see Table S1 in Trageser et al., 2009)
V_H-DJ_H junctions in Ph^+ ALL (see Table S1 in Trageser et al., 2009)

V_H-DJ_H junctions in ETV6-RUNX1 ALL: 4/13 *ETV6-RUNX1* ALL cases (30.8%)

ETV6-RUNX1 I	CTTGMVRGV#LYYYYGMD
ETV6-RUNX1 II	#VREGTSGAKG
ETV6-RUNX1 III	CAHRPNIRYDAFDIW
ETV6-RUNX1 IV	CARGKWIRHYYYYMDVW
ETV6-RUNX1 V	CAREG**WEPPMLLIYYYG
ETV6-RUNX1 VI	CARDSLRYFDWLG#DYW
ETV6-RUNX1 VII	CARIQRYYYMDVW
ETV6-RUNX1 VIII	CQEKGPA*YYYMD
	PSL*LLGPRNPGH
ETV6-RUNX1 IX	L*QLV*L
ETV6-RUNX1 X	CPVRRLLYYY*GMDV
ETV6-RUNX1 XI	CTR*DL*VSAPSSW#DYW
	CARIWGWGGVGGAARRG
ETV6-RUNX1 XII	CP*TYYDILTGYYYYYYGMRRL
ETV6-RUNX1 XIII	CDEFGWW*LLPSLT

V_H-DJ_H junctions in Hyperdiploid ALL: 1/30 Hyperdiploid ALL cases (3.3%)

Hyperdiploid I	CARVPSIVVVPAADGITTTTTVWT##
Hyperdiploid II	H*DIVVVPAAIHYYYGMDV
Hyperdiploid III	CAKDIIDRWE##YFDYW
Hyperdiploid IV	CARGGGFG#YYGMDVW
Hyperdiploid V	CAKDLRE*YQL#YYYYYGMDVW
Hyperdiploid VI	CAHLLPERNS*TYMVRGVIIRKPPYYYYGMDV
Hyperdiploid VII	CARCRSFCIAVA#YFDYW
Hyperdiploid VIII	CARETVGI#PFDYW
Hyperdiploid IX	CARV*V*LRLGELSIE#SDYW
Hyperdiploid X	CAR#FDYW
Hyperdiploid XII	CAHRPNSFSSSGGSC#*DYW
Hyperdiploid XIII	CARGHQS*LG*PWADYW
Hyperdiploid XIV	CARDRIAARP*#W
	CARDAVLMVYAIR##NGMDVW
Hyperdiploid XV	CARDPGMVRGVRPTTTTVW
Hyperdiploid XVI	SPSPQ#
Hyperdiploid XVII	GRGVL*WW*LLLGPWGQG
Hyperdiploid XVIII	PPVSGY*RSGLWLLLLRYGRLGPR
Hyperdiploid XIX	CAR#*LLYYFDYW
Hyperdiploid XX	CAKDYVLRFLEQ*#WLLYYYYGMDVW
Hyperdiploid XXI	CASSTIFGVVTSYYY
Hyperdiploid XXII	CARDRGLTESLRYFDWLLWAS#DPW
Hyperdiploid XXIII	CASDGPSGGD*LGI##DYW
Hyperdiploid XXIV	CAKGNPWDDFWSGYYR#NWFDPW
Hyperdiploid XXV	CARGLGATG#YYYYYYMDVW
Hyperdiploid XXVI	CARDSAGCGSSTSCYRG#AFDIW
Hyperdiploid XXVII	CASRGYASHM#YYYYYVDFW
Hyperd. XXVIII	YIVVVTAT*TGTSI
Hyperdiploid XXIX	CARDGPGDGR*LGT
Hyperdiploid XXX	CARPHYSNYV#YYYYYGMDVW
	CARGGRTVTTSY*YYYGMDV

Note: grey shades denote non-functional rearrangements; * Stop codon; # frame shift

V_H-DJ_H junctions in MLL-AF4 ALL: 0/7 *MLL-AF4* cases (0%)

MLL-AF4 I	CARGFERVL**YQL#YYYYYYMDVW
	CARDVLL***WLLPGYYYYYYGMDV
	CARDPYSSGWYYYDSSGYYQ#YYYYYYG
MLL-AF4 II	CARD*SRY*WCMLY##WFDPW
MLL-AF4 III	CAHRWDFITMVRGVIIP#YYYYGMDVW
MLL-AF4 IV	CARLL*WW*LPP#YYYYGMDVW
MLL-AF4 V	LC#RTG***GVLLLLRYGTFG
	LCESKTTVTTQVRPLGP#NWFD
MLL-AF4 VI	CARDLL**LLPGDYYGMDVW
MLL-AF4 VII	SELT*NWFDPW

V_H-DJ_H junctions in TCF3-PBX1 ALL: 8/8 *TCF3-PBX1* ALL cases (100%)

TCF3-PBX1 I	SVREAPPFVAETFQDWGQGHW
TCF3-PBX1 II	CARGSDDYGDYVAPGGRDQDFD
TCF3-PBX1 III	CTTLGGGGFLDQSAAWFD
TCF3-PBX1 IV	CARIRPYCSSTSCYNEST
TCF3-PBX1 V	CARDPRRVLWFGELT
TCF3-PBX1 VI	CAREHPLVRFG*MLL***WLLVN
	CARDFYWGSDYDAFDI
TCF3-PBX1 VII	CAREGSIVVVPAATS*YYFDY
	CARGHPRFLEWLLYRYYFDY
TCF3-PBX1 VIII	CAREHPLVRYYLLDVW

V_H-DJ_H junctions in ALL with normal karyotype: 8/33 ALL cases with normal karyotype (24.2%)

Normal Karyotype I	CARPEEAYLITMVRGVIMVPTGARTLG#
Normal Karyotype II	CARDDGPYGMDR##
Normal Karyotype III	CARDLG*LGMTTGARAP
Normal Karyotype IV	CARIERFG#FDYW
Normal Karyotype V	CARPQEKQ#YYYYGMDVW
Normal Karyotype VI	YCSSTSCYSLNH*L
Normal Karyotype VII	CPVRRLLLLLRYGR
Normal Karyotype VIII	CARVSHSSGSP#YWYFDLW
Normal Karyotype IX	CARCGYHSSGYYYGTAVHYW
Normal Karyotype X	TTWTSGARA
Normal Karyotype XII	CARGGY#WFDPW
Normal Karyotype XIII	CARAPPYGYCSSTSCYGK#YYYGMDVW
	CAPPLRYFDW*LFRRRT
Normal Karyotype XIV	CAKDPQQ#FDYW
	CARDKVWIAAA#YYYYYGMDVW
Normal Karyotype XV	C*PGGYYF#YYYYYYMDVW
Normal Karyotype XVI	CAHSPFAGALFDY*GQG
Normal Karyotype XVII	CARGEGYYDFWSGYYTG
Normal Karyotype XVIII	CVRGRSGW#YW
Normal Karyotype XIX	CARDLG#FDPW
Normal Karyotype XX	CVR*RTREEIFGSAAGS
Normal Karyotype XXI	CARASVVTA#W
Normal Karyotype XXII	CARGYGGMD
Normal Karyotype XXIII	CARGPHLDIRCSSTSCYGSGSYYLTTGAR
Normal Karyotype XXIV	CARAGTIKRYFDWLL*SIMITFGGVI#F
Normal Karyotype XXV	CAKGLPLKTDF##IDYW
Normal Karyotype XXVI	TGAREPLVTVSSG
Normal Karyotype XXVII	CAKPLLL***WLLK#CFDYW
Normal Karyotype XXVIII	CARAGGGPSPYYYGMDVW
Normal Karyotype XXIX	CARGGDCSGG##CYSGAPHYYYYYMDV
Normal Karyotype XXX	CTTDLVVVPAAMPHL*#W
Normal Karyotype XXXI	CVREYYDSSGCLA#DYW
Normal Karyotype XXXII	CARDRVIGGGFFTYYYDSSGYYYVP#YY
Normal Karyotype XXXIII	CARDPKPAARPDTIF*L

Table S5. Related to Figure 2. Overview of pre-BCR^{-} and pre-BCR^{+} ALL cases studied (n=830)

Studies	**# cases**	**pre-BCR^{-}**	***MLL***	***Ph*$^{+}$**	***RUNX1***	**Hyperdipl**	**Other**	***PBX*1**	**6q21**	**1q23**
St Jude	118	95	19	15	20	17	24	0	0	0
P9906	207	178	20	22	3	0	129	4	0	0
ECOG	191	172	25	78	0	0	69	0	0	0
MDACC	208	182	14	58	0	16	94	0	0	0
UCSF	68	59	0	7	6	8	38	0	0	0
Cell lines	16	11	3	4	1	0	3	0	0	0
Xenografts	22	21	2	12	1	0	6	0	0	0
Sum	**830**	**718**	**83**	**196**	**31**	**41**	**363**	**4**	**0**	**0**
%		86.5	11.6	27.3	4.3	5.7	50.6	0.6	0	0
Studies	**# cases**	**pre-BCR^{+}**	***MLL***	***Ph*$^{+}$**	***RUNX1***	**Hyperdipl**	**Other**	***PBX*1**	**6q21**	**1q23**
St Jude	118	23	1	0	0	0	4	18	0	0
P9906	207	29	1	0	0	0	9	19	0	0
ECOG	191	19	0	0	0	0	13	6	0	0
MDACC	208	26	1	0	0	1	16	3	3	2
UCSF	68	9	0	0	0	1	1	2	3	2
Cell lines	16	5	0	0	0	0	0	4	1	0
Xenografts	22	1	0	0	0	0	0	1	0	0
Sum	**830**	**112**	**3**	**0**	**0**	**2**	**43**	**53**	**7**	**4**
%		13.5	2.7	0	0	1.8	38.4	47.3	6.3	3.6
		Total	***MLL***	***Ph*$^{+}$**	***RUNX1***	**Hyperdipl**	**Other**	***PBX*1**	**6q21**	**1q23**
# cases		**830**	**86**	**196**	**31**	**43**	**406**	**57**	**7**	**4**
Ratio	**pre-BCR^{-}**	86.5	96.5	100	100	95.3	89.4	7	0	0
	pre-BCR^{+}	13.5	3.5	0	0	4.7	10.6	93	100	100

Note: St. Jude, COG P9906 and ECOG E2993 patient microarray data were downloaded from GEO database with the accession numbers provided in the Supplemental Experimental Procedures.

Table S6. Related to Figure 2. Distribution of pre-BCR^{-} and pre-BCR^{+} ALL cases with Age, WBC and Sex

		COG			ECOG			MDACC		
		pre-BCR^{+}	pre-BCR^{-}	p value	pre-BCR^{+}	pre-BCR^{-}	p value	pre-BCR^{+}	pre-BCR^{-}	p value
Age	Mean (min-max, years)	10.45 (2.4-20.4)	11.25 (1.1-19.3)	0.585	36.8 (18-60)	40.5 (17-63)	0.247	40.3 (2.9-77)	41.3 (1.1-80)	0.829
WBC	Mean (10^3/ml)	116	112	0.868	83.3	70.5	0.611	42.6	46.2	0.901
Sex	Male	15	122		12	97		10	105	
	Female	14	56	0.0913	7	75	0.633	16	77	0.0906

WBC: white blood count; P values were calculated from Fisher's exact test for Sex and from t-test for Age and WBC.

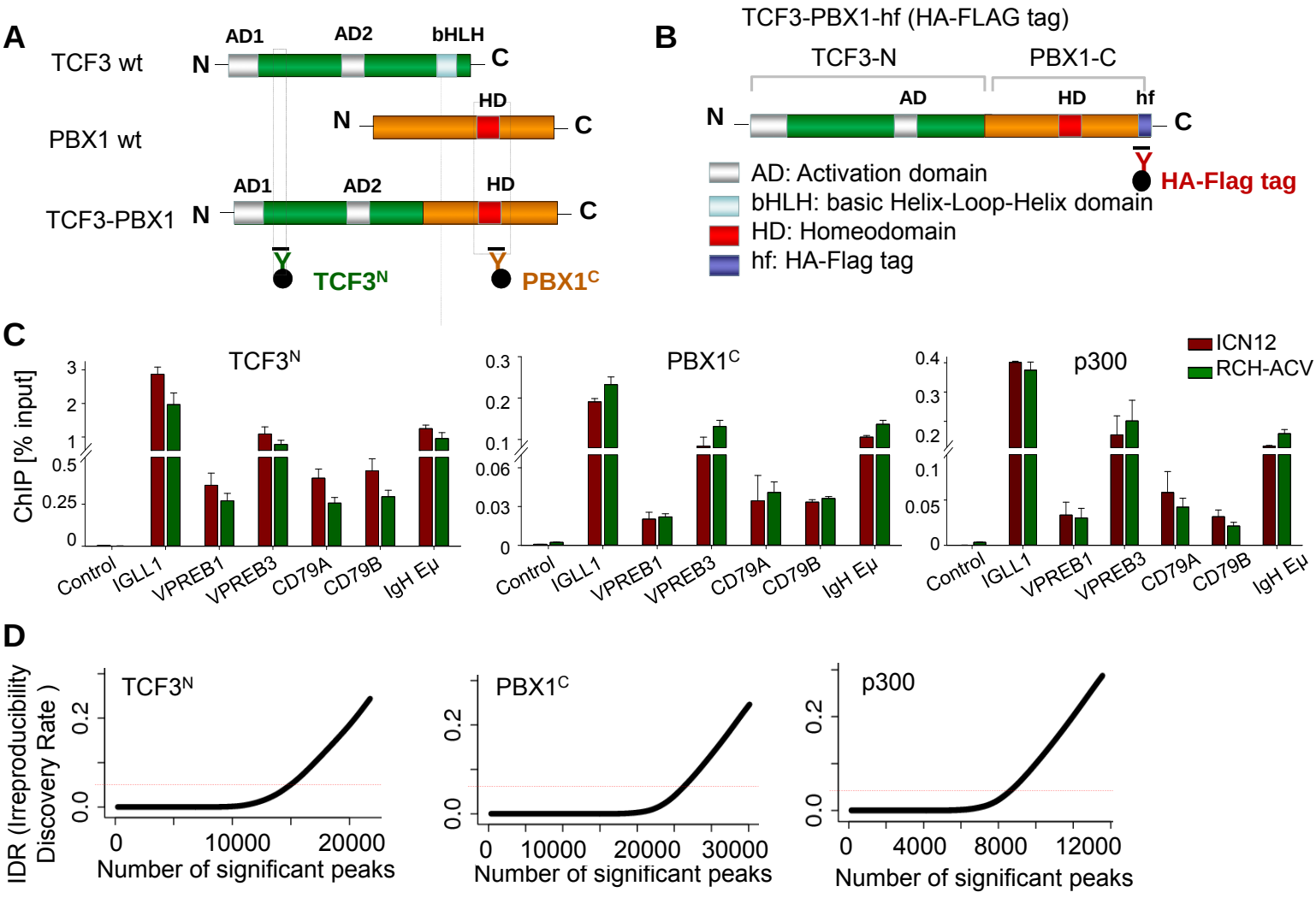

E

ChIP-seq experiemnt	Total reads	Uniquely aligned reads	Number of peaks detected IDR**<=0.05	IDR<=0.1	ChIPseeqer parameters
TCF3^{N} ICN12	42,832,976	37,285,298	14,966	17,034	-t 15 -f 2 –fraglen 170
PBX1^{C} ICN12	71,539,556	54,779,120	25,612	28,370	-t 15 -f 2 -fraglen 170
p300 ICN12	54,629,598	46,401,734	8,857	10,005	-t 15 -f 2 -fraglen 170
Input ICN12	72,568,562	59,893,767			

F

Targets	Chrom	Start	End	IDR TCF3^{N}	IDR PBX1^{C}	IDR p300
IGLL1	chr22	22,251,022	22,256,883	0.002296	7.36E-07	6.32E-08
VpreB1	chr22	20,927,192	20,930,122	2.23E-06	8.52E-07	2.46E-07
VpreB3	chr22	22,424,064	22,426,994	1.42E-06	2.70E-06	2.25E-06
CD79A	chr19	47,070,776	47,074,539	8.83E-06	1.00E-06	3.49E-06
CD79B	chr17	59,357,830	59,365,436	2.90E-06	1.16E-06	2.18E-06
IGHM Eμ	chr14	105,398,977	105,399,760	6.08E-06	7.26E-07	1.14E-06
BLK	chr8	11,386,639	11,387,916	5.83E-06	2.11E-06	5.66E-06
BANK1	chr4	102,930,393	102,931,206	5.03E-06	8.39E-07	4.39E-06

Figure S2. Related to Figure 3. Graphical representations of TCF3-PBX1 ChIP-seq and QChIP validation. (**A**) Graphical representations of ChIP for TCF3 N-terminal ($TCF3^{N}$), PBX1 C-terminal ($PBX1^{C}$) and TCF3-PBX1 fusion protein. (**B**) Inducible expression of TCF3-PBX1-hf with an HA-Flag tag for the fusion-specific ChIP. (**C**) QChIP validation on pre-BCR genes using antibodies for $TCF3^{N}$, $PBX1^{C}$ and p300 in *TCF3-PBX1* ALL cells RCH-ACV and ICN12. Y axis represents ChIP enrichment relative to input. An inactive intragenic region serves as a negative control. Data represent means ± SEM (n=3). (**D**) To estimate self-consistency and determine appropriate thresholds for binding sites peak calling, Irreproducibility Discovery Rate (IDR) analysis (Li et al. 2011; Landt et al. 2012) were performed for each mapped sample. The peaks under IDR 0.05 for each sample is considered as reproducible significant peaks. (**E**) Summary of number of reads and peaks detected in each ChIP-seq experiment. Peaks called by ChIPseeqer program (Giannopoulou and Elemento, 2011) and peak threshold determined by IDR. (**F**) IDR values for the TCF3-PBX1 target genes.

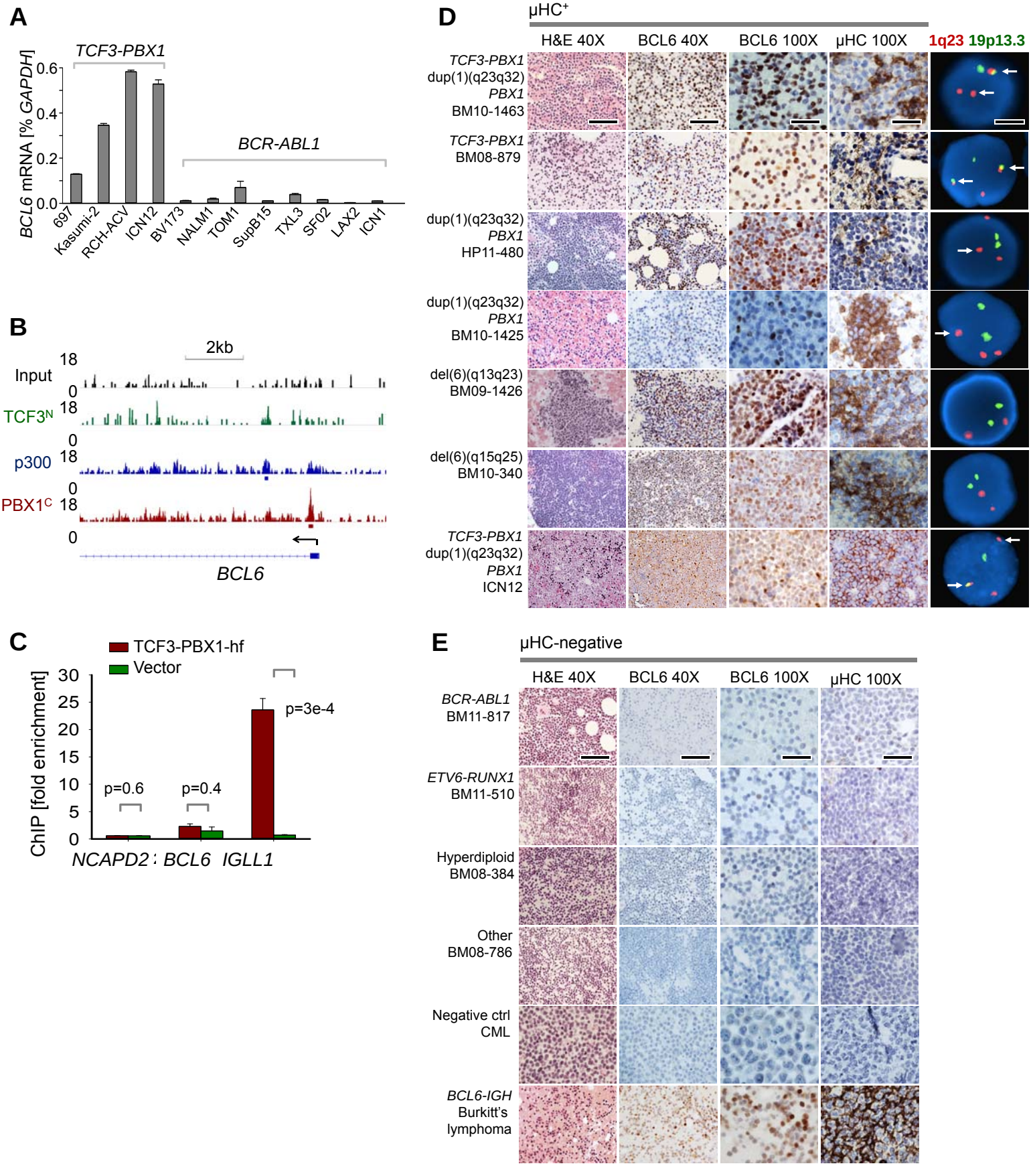
A
TCF3-PBX1
BCR-ABL1
BCL6 mRNA [% GAPDH]
0.6
0.4
0.2
0.0
697
Kasumi-2
RCH-ACV
ICN12
BV173
NALM1
TOM1
SupB15
TXL3
SF02
LAX2
ICN1
B
2kb
Input
TCF3N
p300
PBX1C
18
0
BCL6
C
TCF3-PBX1-hf
Vector
ChIP [fold enrichment]
30
25
20
15
10
5
0
p=0.6
p=0.4
p=3e-4
NCAPD2
BCL6
IGLL1
D
μHC+
H&E 40X
BCL6 40X
BCL6 100X
μHC 100X
1q23 19p13.3
TCF3-PBX1
dup(1)(q23q32)
PBX1
BM10-1463
TCF3-PBX1
BM08-879
dup(1)(q23q32)
PBX1
HP11-480
dup(1)(q23q32)
PBX1
BM10-1425
del(6)(q13q23)
BM09-1426
del(6)(q15q25)
BM10-340
TCF3-PBX1
dup(1)(q23q32)
PBX1
ICN12
E
μHC-negative
H&E 40X
BCL6 40X
BCL6 100X
μHC 100X
BCR-ABL1
BM11-817
ETV6-RUNX1
BM11-510
Hyperdiploid
BM08-384
Other
BM08-786
Negative ctrl
CML
BCL6-IGH
Burkitt's
lymphoma

Figure S3. Related to Figure 4. BCL6 is expressed in pre-BCR^{+} but not pre-BCR^{-} ALL cells. (**A**) *BCL6* mRNA expression levels were measured by qRT-PCR with *GAPDH* as control on pre-B ALL samples. Data represent means ± SEM (n=3). (**B**) ChIP-seq tracks for TCF3^{N}, PBX1^{C} and p300 antibodies vs. input on the BCL6 locus in *TCF3-PBX1* ALL cells (ICN12). The gene models were shown in UCSC genome browser view hg18. (**C**) QChIP validation using the antibody against the TCF3-PBX1-hf tag vs. an empty vector control on *BCL6*, with *IGLL1* as a positive and *NCAPD2* as a negative control. Data represent means ± SEM (n=3). P values from t-test. (**D-E**) Hematoxylin and eosin (H&E) staining and immunohistochemistry for BCL6 and cytoplasmic μHC were performed on paraffin-embedded bone marrow samples from pre-B ALL patients (UCSF, n=72). A Burkett lymphoma and a CML sample were used as a positive and negative control. FISH images validated *TCF3-PBX1* gene rearrangement or gain of 1q23 encompassing the *PBX1* locus in respective ALL patient samples. Scale bars, 125 μm (H&E), 125 μM, 50 μm and 50 μm (immunohistochemistry, from left to right panels) or 5 μm (FISH).

Table S7. Related to Figure 4. Pre-B ALL patient samples (UCSF, n=72) studied by immunohistochemistry

Case	Cytogenetics	Subtypes	Clinical course	Sex Age	CD19	CD34	TdT	CD79A	μHC	BCL6
BM10-1463	t(1;19)(q23;p13.3)	*TCF3-PBX1*	diagnosis	m/53	+	-	+	-	+	+
BM08-879	t(1;19)(q23;p13.3)	*TCF3-PBX1*	diagnosis	f/9	+	-	+	+	+	+
BM04-137	t(1;19)(q23;p13.3)	*TCF3-PBX1*	diagnosis	f/27	+	-	+	+	+	+
BM07-117	t(1;19)(q23;p13.3)	*TCF3-PBX1*	diagnosis	f/1	+	-	-	+	+	+
BM07-554	t(1;19)(q23;p13.3)	*TCF3-PBX1*	diagnosis	m/73	+	-	-	+	+	+
HP11-480	dup(1)(q23q32)	1q gain (*PBX1*)	diagnosis	m/73	+	-	-	+	+	+
BM10-340	-7, del(6)(q15q25), add(9)(p13),del(9)(p21),-20	del(6)(q21)	diagnosis	m/36	+	-	+	+	+	+
BM09-1426	hypodiploid 37,XY,-2,-3,-4,-5, del(6)(q13q23), add(11)(q25),-12,-13,-14,-16,-	Hypodiploid, del(6)(q21)	diagnosis	m/13	+	-	+	+	+	+
BM08-746		Hyperdiploid	diagnosis	m/4	+	-	+	+	+	+
HP12-71	54,XY,+X,+4,+6,+14,?i(17)(q10),+18,+21,+21	Other	diagnosis	m/4	+	-	+	+	+	+
HP12-802	45,XX, dic (12;14)(p11.1:q13)	Other	diagnosis	f/2	+	-	+	-	+	+
HP13-1026	46,XX,+X,-7, del(9)(p21),add(20)(p13)	Other	diagnosis	f/37	+	-	+	+	+	+
BM11-817	t(9;22)	*BCR-ABL1*	diagnosis	f/63	+	+	+	-	-	-
BM08-399	t(9;22)	*BCR-ABL1*	diagnosis	m/25	+	+	+	+	-	-
BM08-1187	t(9;22), -7, b2a2	*BCR-ABL1*	diagnosis	m/68	+	+	+	+	-	-
HP11-249	46,XX,t(9;22)(q34;q11)	*BCR-ABL1*	diagnosis	f/52	+	+	+	-	-	-
HP13-544	46, XY, t(9;22)(q34;q11.2)	*BCR-ABL1*	diagnosis	m/47	+	+	+	+	-	-
BM10-1136	44,X,-X,-7,t(9;22)	*BCR-ABL1*	diagnosis	f/43	+	+	+	-	-	-
BM11-409	t(9;22), p210+	*BCR-ABL1*	diagnosis	f/32	+	+	+	-	-	-
HP11-661	t(12;21), 46,XX normal	*ETV6-RUNX1*	diagnosis	f/4	+	+	+	+	-	-
HP11-907	t(12;21),46,XY,add(4)(q35),der(6)t(6;17)(q13;q11.2),del(12)(p11.2p13),17,+mar[13]/47,XY,add(4)(p16),der(6)t(6;17)(q13;q11.2),-17,+?16, +mar[2]/46,XY[5]	*ETV6-RUNX1*	diagnosis	m/3	+	+	+	+	-	-
BM11-173	t(12;21)	*ETV6-RUNX1*	diagnosis	f/3	+	+	+	-	-	-
BM11-413	t(12;21)	*ETV6-RUNX1*	diagnosis	m/2	+	+	+	+	-	-
BM11-510	t(12;21)	*ETV6-RUNX1*	diagnosis	m/4	+	+	+	-	-	-
BM11-755	t(12;21)	*ETV6-RUNX1*	diagnosis	f/8	+	+	+	-	-	-
BM08-384		hyperdiploid	diagnosis	m/2	+	+	+	-	-	-
BM08-1174		hyperdiploid	diagnosis	f/3	+	+	+	+	-	-
BM09-678		hyperdiploid	diagnosis	m/10	+	+	+	+	-	-
BM09-1511		hyperdiploid	diagnosis	m/4	+	+	+	+	-	-
BM09-1303		hyperdiploid	diagnosis	m/6	+	+	+	+	-	-
BM10-332		hyperdiploid	diagnosis	f/5	+	+	+	+	-	-
BM08-884		hyperdiploid	diagnosis	f/6	+	+	+	+	-	-
BM08-1426		Other	diagnosis	f/35	+	+	+	+	-	-
BM08-387		Other	diagnosis	f/4	+	+	+	-	-	-
BM08-400		Other	diagnosis	m/22	+	+	+	+	-	-
BM08-449		Other	diagnosis	f/3	+	-	+	+	-	-
BM08-501		Other	diagnosis	m/4	+	+	+	-	-	-
BM08-658		Other	diagnosis	m/17	+	+	+	+	-	-
BM08-786		Other	diagnosis	f/16	+	+	+	+	-	-
BM08-877		Other	diagnosis	m/19	+	+	+	+	-	-
BM09-109		Other	diagnosis	f/2	+	+	+	+	+	-
BM09-214	+X,add(8)(p?12),der(20;21)(p10;q10)	Other	diagnosis	m/49	+	+	+	+	-	-
BM09-507		Other	diagnosis	m/20	+	+	+	+	-	-
BM10-1011	+gain AML1	Other	diagnosis	m/3	+	+	+	-	+	-
BM10-1150	+4, 10, 17	Other	diagnosis	m/4	+	+	+	-	-	-
BM10-1156	+X,4,6,10,18,21	Other	diagnosis	m/5	+	+	+	-	-	-
BM10-1187	+4,10,17	Other	diagnosis	f/5	+	+	+	-	-	-
BM10-1337	+4,10,17	Other	diagnosis	m/2	+	+	+	-	-	-
BM10-1373	+4,17 (not 10)	Other	diagnosis	m/2	+	+	+	-	-	-

Case	Cytogenetics	Subtypes	Clinical course	Sex Age	CD19	CD34	TdT	CD79A	μHC	BCL6
BM10-1503		Other	diagnosis	f/56	+	+	+	-	-	-
BM10-1544		Other	diagnosis	f/18	+	-	+	-	-	-
BM10-445		Other	diagnosis	m/0.3	+	+	+	-	-	-
BM10-673	Partial del 9q	Other	diagnosis	m/8	+	+	-	-	-	-
BM11-228	+4,10 (not17)	Other	diagnosis	m/9	+	+	+	-	-	-
BM11-343	+4,10,17	Other	diagnosis	f/3	+	+	+	-	-	-
HP11-24		Other	diagnosis	f/11	+	+	+	-	-	-
HP11-575		Other	diagnosis	f/31	+	+	+	+	-	-
HP11-790		Other	diagnosis	m/29	+	+	+	+	-	-
HP12-1014		Other	Relapse	f/43	+	-	+	+	-	-
HP12-1499	46, XX	Other	diagnosis	f/9	+	-	+	+	-	-
BM10-1425	trisomy 1	Other	diagnosis	f/9	+	+	+	-	-	-
HP12-49	46,XY,t(1;14)(q25;q32),del(4)(q12q?25),del(12)(q21q22),+19[3]/ 46,XY[4]	Other	diagnosis	m/10	+	-	+	+	-	-
HP12-1722	59-60. XY. +4. +5, +6, +8, +1-, +13, +14, +15, +17, +18, +21, +21[cp2]/46, XY [13]	Other	diagnosis	m/2	+	+	+	+	-	-
HP12-1724	46, XX, add(4), (p14)[3]/46,xx[17]	Other	diagnosis	f/14	+	+	+	+	-	-
HP12-446	no cyto division	Other	diagnosis	m/22	+	+	+	+	-	-
HP12-657	46, XY, add(14)(q32)[6]/46,XY [14]	Other	diagnosis	m/20	+	+	+			-
HP12-924		Other	diagnosis	f/3	+	+	-	+	-	-
HP13-135	45,-X, -x?c[6]/46,XX[14].nuc ish (CEP8x2)[194],(RUNX11T1,RUNX1)x2[181],(ABL1,BCR)x2[176],(MLLx2)190	Other	Relapse	f/23	+	+			-	-
HP13-362	46, XY [26]	Other	diagnosis	m/53	+	+	+	+	-	-
HP13-495	46, XY [20]	Other	diagnosis	m/22	+	-	+	+	-	-
HP13-628	54,XY, +X, +4, +6, +8, +14, +17, +21 [cp2]/46,XY[9]	Other	diagnosis	m/1	+	+	+	+	-	-

Table S8. Related to Figure 4. 1q23 abnormalities in human ALL and mature B-cell lymphoma

Rearrangements of 1q23 to Non-TCF3 fusion partners in human ALL

Case	Reference	Karyotype	1q23
3	Harewood 2003, Leukemia17:547-553	46,XY,**t(1;16)(q23;p13),**ider(21)(q10)dup(21)(q?)/51,idem,+X,+3,+10,+14,+21	*PBX1*-rearr.
3	Gutierrez-Angulo 2004, Hematol Oncol 22:85-90	46,XY,**t(1;9)(q23;q34)**	*PBX1*-rearr.
4		46,XY,**t(1;19)(q23;p13)/46**,idem,dup(1)(q23q44)	*PBX1*-rearr.
31	Einerson 2005, Am J Clin Pathol 124:421-429	46,XY,**der(1)t(1;1)(p36;q23),**der(9)t(7;9)(p15;p22),t(14;18)(q32;q21)	*PBX*1-rearr.
1	Bilic 2007, Cancer Genet Cytogenet 172:90-91	46,XX, **der(15)t(1;15)(q23;q26)**	*PBX1*-rearr.
64	Adeyinka 2007, Cancer Genet Cytogenet 173:136-143	45-46,XX,t(9;13)(q21;q22),+13,der(17;21)(q10;q10)/46-47,XX, **t(1;13)(q23;q14)**,del(2)(q34),del(7)(q22q32),+15,add(22)(p11)/45-46,XX, del(2),t(3;14)(p21;q21),del(7), der(13;15)(q10;q10),-14,add(17)(p13), add(22),+mar	*PBX*1-rearr.
3131	Rand 2011, Blood 117:6848-6855	46,XY,**t(1;16)(q23;p13),**ider(21)(q10)dup(21)(q?)/51,idem,+X,+3,+10,+14,+21	*PBX1*-rearr.
1	Inokuchi 2011, Int J Hematol 94:255-260	46,XY,t**(1;9)(q23;q34)**,inv(2)(p21q33)	*PBX*1-rearr.
1	Fonatsch 1982, Int J Cancer 30:321-327	46,XY,del(2)(p21),inv(2)(p11q13),ins(11;3)(q23;p12p21),t(8;22)(q24;q12)/ 46,XY,**dup(1)(q23q44)**,t(8;22)	dup *PBX1*
3	Childs 1988, Hematol Pathol 2:145-157	51,XX,+X,+del(4)(q21),t(4;11)(q21;q23),+6,**der(15)t(1;15)(q23;q26)**,+22,+22	*PBX1*-rearr.
12	Berger 1990, Cancer Genet Cytogenet 44:69-75	46,XY,add(1)(p34),**t(1;14)(q23;q32),**del(2)(p12p23),-3,del(12)(p12)	*PBX*1-rearr.
46	Pui 1992, Blood 79:2384-2391	46,XY,i(7)(q10),**der(19)t(1;19)(q23;p13)/46**,idem,der(22)t(1;22)(q23;p11)	*PBX1*-rearr.
18	Heerema 1992, Leukemia6:185-192	62,XXY,-1,**dup(1)(q23q44)**,-2,-3,-7,-8,-15,-16,-19,-20,+21,+21	dup *PBX*1
708	Secker-Walker 1992, Leukemia 6:363-369	54,XY,+X,+4,+6,+7,+8,+17,**der(19)t(1;19)(q23;p13)**,+21,+21/54,idem,dup (1)(q23q44)	*PBX1*-rearr.
415	Tilly 1994, Blood 84:1043-1049	46,XX,**der(1)t(1;1)(p36;q23),**der(2)dup(2)(p12p25)t(2;18)(p12;q21),add(16)(p11),i(17)(q10)	*PBX*1-rearr.
22	Fegan 1995, Leukemia 9:2003-2008	46,XY,**t(1;13)(q23;q14)**,t(13;14)(q12;q24)	*PBX1*-rearr.
1	Jarvis 1999, Cancer Genet Cytogenet 114:112-116	46,XY,**der(1)t(1;1)(q23;q32)/46**,XY,der(22)t(1;22)(q23;p11)	*PBX*1-rearr.
17	Lim 1999, Int J Mol Med 4:665-667	46-49,XY,**t(1;14)(q23;q32)**,del(7),+18,+21	*PBX1*-rearr.
137	Horsman 2001, Genes Chromosomes Cancer 30:375-382	46,XY,**der(1)t(1;1)(p36;q23)**	*PBX*1-rearr.
1	Carroll 1984, Blood 63:721-724	46,XY,**t(1;19)(q23;q13),**der(19)t(1;19)	*PBX1*-rearr.
2		47,XX,**t(1;19)(q23;q13)**,+8	*PBX*1-rearr.
3		47,XY,+6,**der(19)t(1;19)(q23;q13)**	*PBX1*-rearr.

1q23 abnormalities in mature B-cell lymphoma (n=47)

Case	Reference	Disease	Karyotype	1q23
6	Horsman 2003, Br J Haematol 120:424-433	FL	48,XX,+del(X)(q11q?24),**dup(1)(q21q23)**,+der(3)t(3;14)(q27;q32),t(3;14)	dup *PBX1*
10904	Namiki 2003, Int J Hematol 77:490-498	BL	46,XY,**dup(1)(q23q44)**,t(8;14)(q24;q32)	dup *PBX1*
5850	Cook 2004 , Am J Clin Pathol 121:826-835	FL	45,X,-X,t(14;18)(q32;q21)/45,idem,**dup(1)(q21q23)/90**, idemx2,dup(1)x2	dup *PBX1*
39	Yunis 1984, Cancer Genet Cytogenet 13:17-28	B-NHL	48,XX,**dup(1)(q23q32)**,t(2;19)(p15p23;q13),+3,inv(7)(p15q11),+18,del(19)(q13)	dup *PBX1*
34	Ruminy 2006, Oncogene 25:4947-4954	FL	46,XY,**dup(1)(q12q23)**,t(3;14)(q27;q32),der(9)t(9;9)(p24;q23)	dup *PBX1*
602	Struski 2007, Pathol Biol (Paris) 55:59-72	B-NHL	47,XY,**dup(1)(q23q32)**,+3,del(9)(q11q?32)/48,idem,+mar	dup *PBX1*
11	Tholouli 2009, Blood 114:485-486	BL	46,XY,**dup(1)(q23q32)**,t(8;22)(q24;q32),del(9)(q12q22)	dup *PBX1*
11	Sanger 1987, Cancer 60:3014-3019	FL	67-70,XXX,**dup(1)(q23)**,-2,t(3;6)(q27;q15),-4,+7,+del(7)(q21),-8,t(14;18)(q32;q21),+der(14)t(14;18)x2,-15,-16,+17,-18,-19,+20,-21,-22,+mar	dup *PBX1*
7	Olah 1989 , Cancer Genet Cytogenet 43:179-194	BL	47,XY,t(8;14)(q24;q32),+mar/46,XY,t(2;8)(p13;q23)/47,XY,+del(1)(q12),**dup(1)(q23q32),**t(1;1)(q32;q32)	dup *PBX1*
1	Slater 1979, Int J Cancer 23:639-647	BL	46,XY,**dup(1)(q23q32)**,t(1;6)(q21;q13),del(6)(q13),del(8)(p21),add(14)(q32)	dup *PBX1*
50	Nowotny 1996, Ann Hematol 72:291-301	DLBCL	49,X,-Y,+X,**dup(1)(q23q31)**,+3,del(4)(p16),add(6)(p23), del(6)(q13q35),t(12;14)(q24;q32),+18	dup *PBX1*
60		DLBCL	47,XX,**dup(1)(q23q31)**,t(2;7)(q12;q21),dic(3;6)(q23;q27),+7,add(7)(p22)x2,add(9)(q34),t(12;20)(p10;q10),t(12;16)(q15;q13),-13,+der(19)/47,idem,dic(1;9)(q44;q10),del(13)(q13q31)	dup *PBX1*
2432	Koduru 1997, Blood 90:4078-4091	DLBCL	45,X,add(X)(q21),**add(1)(q23)**,add(2)(p11),del(3)(q13),t(3;14)(q27;q32),i(8)(q10),add(12)(q24),-15	dup *PBX1*
1	Slater 1982, Med Pediatr Oncol 10:71-84	BL	46,XX,**dup(1)(q23q32)**,del(3)(p25),t(8;14)(q24;q32)	dup *PBX1*
15	Fukuhara 1983, Jpn J Clin Oncol 13:461-476	BL	46,XY,**dup(1)(q23q32)**,t(8;14)(q24;q32)	dup *PBX1*
24	Mohamed 2001, Cancer Genet Cytogenet 126:45-51	FL	46,XY,add(1)(p36),t(14;18)(q32;q21)/46,idem,**dup(1)(q23q42)**/47,idem,+2	dup *PBX1*
33		FL	45,X,-Y,**dup(1)(q23q42)**,-4,+7,t(14;18)(q32;q21)	dup *PBX1*
8	Jardin 2002, Leukemia 16:2309-2317	FL	46,XY,**dup(1)(q12q23)**,t(3;14)(q27;q32),der(9)t(9;9)(p24;q23)	dup *PBX1*
12	Kumari 2003, Cancer Genet Cytogenet 141:14-	DLBCL	43-45,XY,-1,**add(1)(q23)**,dup(1)(q21q31),add(2)(p21),	dup *PBX1*

	19		add(18)(q21)
16		DLBCL	47-49,X,-X,**add(1)(q23)**,del(3)(p12)x2,+add(12)(q13),-18,+19,+20,-21,+22,+2mar	dup *PBX1*
67	Bloomfield 1983 , Cancer Res 43:2975-2984	DLBCL	49,XY,del(1)(p36),der(3)t(1;3)(q23;p26),+del(9)(q22),**der(14)t(1;14)(q23;q32)**,+19,+21	*PBX1-IGH*
8136	Cook 2004 , Am J Clin Pathol 121:826-835	FL	87-93,XXYY,**t(1;19)(q23;p13)x2**,del(3)(q21q25)x2,add(4)(q35),-7,inv(9)(p11q13)x2,del(10)(q24)x2,-14,t(14;18)(q32;q21)x2,del(15)(q24)x2,-17,der(19)t(1;19),-20,+2mar	*PBX1*-rearr.
31	Einerson 2005, Am J Clin Pathol 124:421-429	FL	46,XY,**der(1)t(1;1)(p36;q23)**,der(9)t(7;9)(p15;p22),t(14;18)(q32;q21)	*PBX1*-rearr.
1	Li 2006 , Cancer Genet Cytogenet 170:140-146	BL	47-48,XY,t(3;14;18),add(4)(q35),add(6)(q27),**der(13)t(1;13)(q23;q34)**,+18	*PBX1*-rearr.
64	Adeyinka 2007, Cancer Genet Cytogenet 173:136-143	CLL	45-46,XX,t(9;13)(q21;q22),+13,der(17;21)(q10;q10)/46-47,XX,**t(1;13)(q23;q14)**,del(2)(q34),del(7)(q22q32),+15,add(22)(p11)/45-46,XX,del(2),t(3;14)(p21;q21),del(7),der(13;15)(q10;q10),-14,add(17)(p13),add(22),+mar	*PBX1*-rearr.
3	Berger 1989, Genes Chromosomes Cancer 1:115-118	BL	46,XY,t(8;14)(q24;q32),der(13)t(3;13)(?;q34)/46,XY,t(8;14),**der(13)t(1;13)(q23;q34)ins(13;?)(q34;?)**	*PBX1*-rearr.
4		BL	46,XX,t(8;14)(q24;q32)/46,idem,**der(13)t(1;13)(q23;q34)**	*PBX1*-rearr.
10	Mark 1979 , Cancer Genet Cytogenet 1:39-56	DLBCL	82,XX,-X,del(X)(q13),+i(1)(p10)x2,+i(1)(q10),-2,-3,-5,del(7)(p11)x2,-8,-8,i(9)(p10),-10,-12,-13,+del(14)(q22),**der(14)t(1;14)(q23;q32)x4**,-15,i(15)(q10),-16,-16,-16,i(17)(q10),-19,-19,-20,+2mar	*PBX1*-rearr.
415	Tilly 1994, Blood 84:1043-1049	FL	46,XX,**der(1)t(1;1)(p36;q23)**,der(2)dup(2)(p12p25)t(2;18)(p12;q21),add(16)(p11),i(17)(q10),der(18)t(2;18)/46,XX,der(1)t(1;1),der(2)dup(2)t(2;18),t(4;15)(q21;q11),add(11)(q23),t(13;16)(q14;p12),i(17)(q10),der(18)t(2;18)	*PBX1*-rearr.
22	Fegan 1995, Leukemia 9:2003-2008	CLL	46,XY,**t(1;13)(q23;q14)**,t(13;14)(q12;q24)	*PBX1*-rearr.
1	Meckenstock 1997 , Leuk Lymphoma 26:197-204	B-NHL	47,XY,+3/47,idem,**der(1)t(1;1)(p36;q23)/46,idem**,-Y,der(1)	*PBX1*-rearr.
51	Dave 1999 , Clin Cancer Res 5:1401-1409	B-NHL	52,XY,**der(1)t(1;1)(p36;q23)**,+5,+7,+13,t(14;18)(q32;q21),+18,+der(18)t(14;18),+mar	*PBX1*-rearr.
14	Fukuhara 1983, Jpn J Clin Oncol 13:461-476	BL	46,X,**der(X)t(X;1)(p11;q23)**,t(8;14)(q24;q32)/47,idem,+mar/46,XX,dup(1)(q23q32),t(8;14)	*PBX1*-rearr.
137	Horsman 2001, Genes Chromosomes Cancer 30:375-382	FL	46,XY,t(14;18)(q32;q21)/46,idem,**der(1)t(1;1)(p36;q23)**	*PBX1*-rearr.
1	Murphy 1984, N Engl J Med 311:195-196	BL	46,XY,t(8;14)(q24;q32)/46,idem,add(1)(q?)/46,idem,**der(19)t(1;19)(q23;p13**)	*TCF3-PBX1*
2	Wlodarska 1994 , Genes Chromosomes Cancer 10:171-176	BL	47,XY,+1,add(2)(p25),t(8;14)(q24;q32),del(13)(q21q31),t(14;18)(q32;q21),del(17)(p12),t(20;22)(q13;q11)/47,idem,del(19)(p12)/47,idem,**der(19)t(1;19)(q23;p13)**	*TCF3-PBX1*
1	Lessard 1994, Leuk Lymphoma 11:149-152	BL	50,XY,**t(1;19)(q23;p13)**,+4,+8,del(9)(p?),+10,del(12)(p?),+17	*TCF3-PBX1*
3		BL	46,XX,**t(1;19)(q23;p13)**	*TCF3-PBX1*
4		BL	51,XY,**t(1;19)(q23;p13)**,+5,+8,+10,+21,+22	*TCF3-PBX1*
5		BL	46,XY,**t(1;19)(q23;p13)**,t(1;17)	*TCF3-PBX1*
5	Devaraj 1995, Leukemia 9:821-825	BL	46,XY,?dup(7)(q11q22),t(8;14)(q24;q32)/46,idem,?dup(10)(q11q26)/46,XY,?trp(7)(q11q22),t(8;14),**der(19)t(1;19)(q23;p13)add(1)(q?)**	*TCF3-PBX1*
3	Khokhar 1995, Cancer Genet Cytogenet 83:18-24	FL	47,XY,t(1;19)(q23;p13),+del(3)(p21),dup(11)(q13q25),**der(19)t(1;19)(q?;p13)**	*TCF3-PBX1*
1	Troussard 1995 , Br J Haematol 89:516-526	BL	47,XX,**t(1;19)(q23;p13)**,+8,del(9)(p22)	*TCF3-PBX1*
8		BL	47,XX,**t(1;19)(q23;p13)**,+8/46,XX,der(19)t(1;19)	*TCF3-PBX1*
50	Petkovic 1996, Cancer Genet Cytogenet 88:57-65	BL	46,XX,t(7;13)(p2?;q2?),**der(19)t(1;19)(q23;p13)/47**,idem,+mar	*TCF3-PBX1*
1	Ichinohasama 2000 , Leukemia 14:169-182	DLBCL	66-82,XXYY,-1,del(1)(p32),dup(1)(q23),i(1)(q10),-2,add(2)(q10),add(3)(p11),+der(3)add(3)t(3;18)(q27;q21),t(3;18)x3,-4,der(4)t(4;22)(p16;q11)del(4)(q31),der(4)t(4;22)add(4)(q35), -5,-6,del(6)(p21)x2,der(6)t(6;14)(q15;q11), -7,-7,-8,add(8)(p23),-9,-10,der(11)t(?6;11)(p11;q12)x2,del(12)(p13)x2,add(13)(q34),der(14)t(X;14)(q13;q32),-15,add(17)(p11),add(19)(q13),**der(19)t(1;19)(q23;p13)**,add(20)(q23),-21,der(22)t(4;22),+mar	*TCF3-PBX1*
12	Velangi 2002, J Clin Pathol 55:591-595	BL	47,XY,add(1)(p36),add(3)(q2?3),+7,t(14;18)(q32;q22),t(15;22)(q26;q21),**der(19)t(1;19)(q23;p13)**	*TCF3-PBX1*
54	López 2013, Genes Chromosomes Cancer 52:920-927	CLL	46,XY,**t(1;19)(q23;p13)**,der(7),+12,del(13)(q14q21),add(15)(p10),del(17) (p12)/46,XY,t(11;14)(q13;q32)	*TCF3-PBX1*

Note: DLBCL: Diffuse large B-cell lymphoma; FL: Follicular lymphoma; BL: Burkitt's lymphoma; CLL: Chronic lymphocytic leukemia. B-NHL, B cell Non-Hodkin's lymphoma. The data were curated from Mitelman Database of Chromosome Aberrations and Gene Fusions in Cancer http://cgap.nci.nih.gov/Chromosomes/Mitelman

A

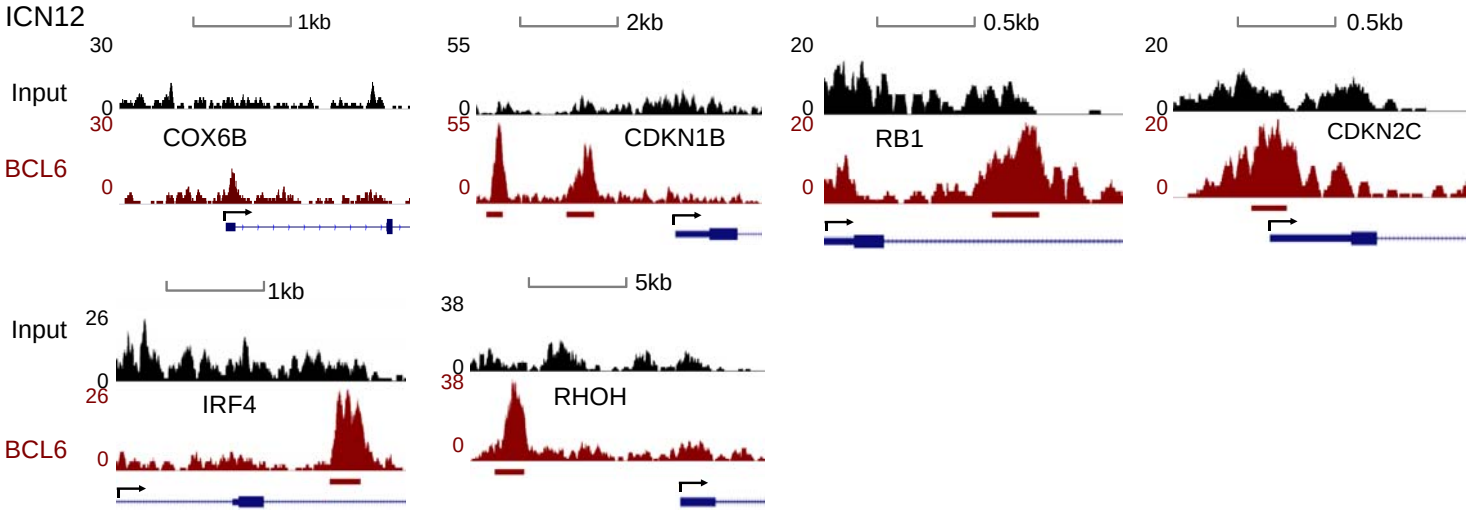

B

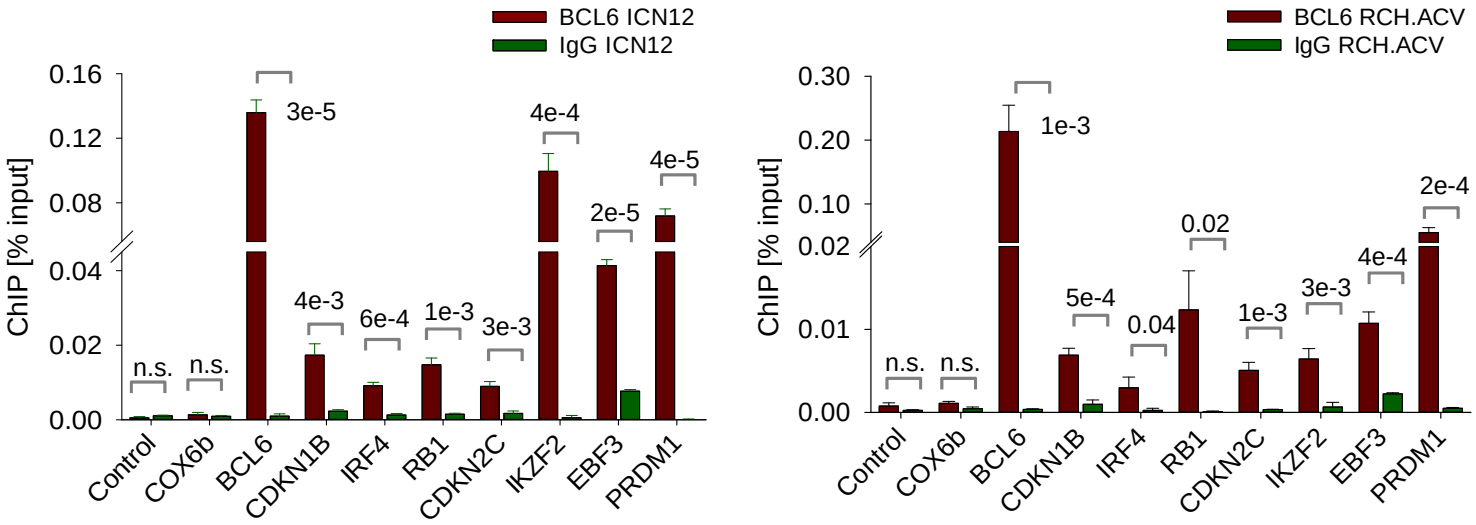

C

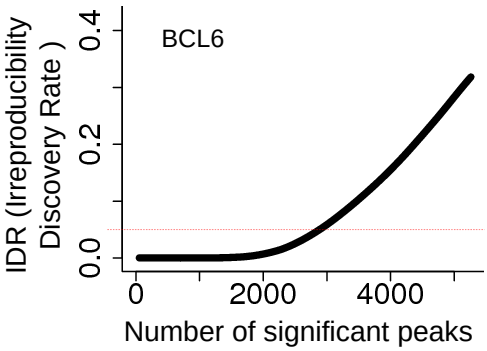

D

ChIP-seq experiment	Total reads	Uniquely aligned reads	Number of peaks detected IDR**<=0.05	DR<=0.1	ChIPseeqer parameters
BCL6 (ICN12)	56,894,092	49,289,096	2,885	3,467	-t 15 -f 2 -fraglen 170
Input (ICN12)	48,961,598	38,399,594			

Figure S4. Related to Figure 5. BCL6 directly binds to a number of pre-BCR check point molecules. (**A**) BCL6 ChIP-seq binding tracks on the target genes including pre-BCR checkpoint molecules (*RB1*, *CDKN2C*, *CDKN1B and IRF4*) in patient-derived *TCF3-PBX1* ALL cells (ICN12). Y axis represents the number of reads for peak summit normalized by the total number of reads per track. Gene models were shown in UCSC genome browser view hg18. The peak regions were called by ChIPseeqer program (Giannopoulou and Elemento, 2011). (**B**) QChIP validation on some BCL6 target genes using antibodies against BCL6 with IgG as a control in *TCF3-PBX1* ALL cells (ICN12 and RCH-ACV). An inactive intragenic control region and COX6b were used as negative controls. Y axis represents ChIP enrichment relative to input. Data represents means ± SEM (n=3). P values from t-test. n.s. means non-significant ($p>0.05$). (**C**) To estimate self-consistency and determine appropriate thresholds for binding sites peak calling, Irreproducibility Discovery Rate (IDR) analysis (Li et al. 2011; Landt et al. 2012) were performed for each mapped sample. The peaks under IDR 0.05 for each sample is considered as reproducible significant peaks. (**D**) Summary of number of reads and peaks detected in the BCL6 ChIP-seq experiment. Reads were aligned to hg18 using BWA with the default parameters (Li et al., 2009). Peaks called by ChIPseeqer program (Giannopoulou and Elemento, 2011). Peak threshold was determined by IDR (Li et al. 2011).

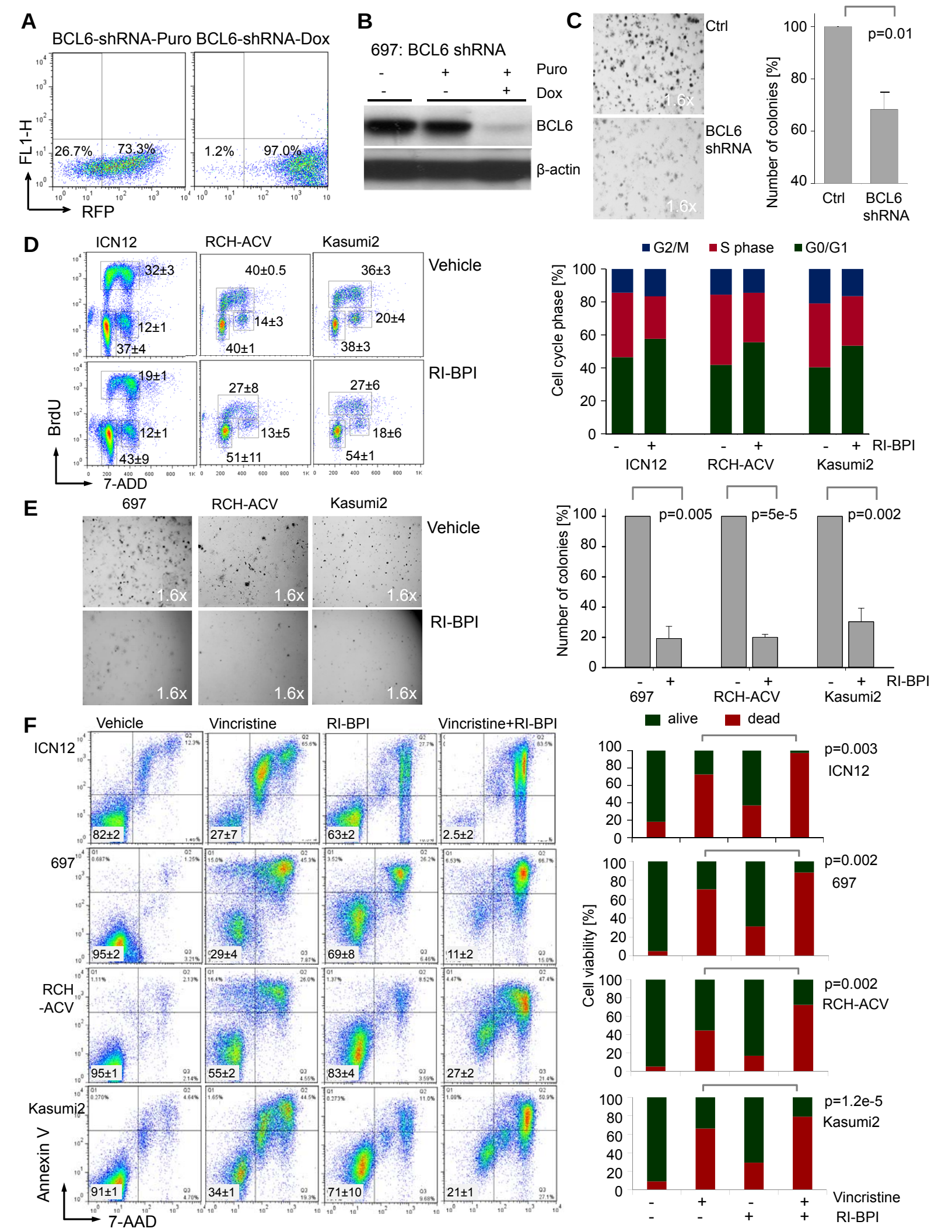
A
BCL6-shRNA-Puro BCL6-shRNA-Dox
FL1-H
RFP
26.7%
73.3%
1.2%
97.0%
B
697: BCL6 shRNA
Puro
Dox
BCL6
β-actin
C
Ctrl
BCL6 shRNA
1.6x
Number of colonies [%]
p=0.01
Ctrl
BCL6 shRNA
D
ICN12
RCH-ACV
Kasumi2
Vehicle
RI-BPI
BrdU
7-ADD
32±3
12±1
37±4
40±0.5
14±3
40±1
36±3
20±4
38±3
19±1
12±1
43±9
27±8
13±5
51±11
27±6
18±6
54±1
G2/M
S phase
G0/G1
Cell cycle phase [%]
RI-BPI
ICN12
RCH-ACV
Kasumi2
E
697
RCH-ACV
Kasumi2
Vehicle
RI-BPI
1.6x
Number of colonies [%]
p=0.005
p=5e-5
p=0.002
RI-BPI
697
RCH-ACV
Kasumi2
F
Vehicle
Vincristine
RI-BPI
Vincristine+RI-BPI
ICN12
697
RCH-ACV
Kasumi2
Annexin V
7-AAD
82±2
27±7
63±2
2.5±2
95±2
29±4
69±8
11±2
95±1
55±2
83±4
27±2
91±1
34±1
71±10
21±1
alive
dead
Cell viability [%]
p=0.003
ICN12
p=0.002
697
p=0.002
RCH-ACV
p=1.2e-5
Kasumi2
Vincristine
RI-BPI

Figure S5. Related to Figure 6. Inhibition of BCL6 via BCL6 shRNA and retro-inverso BCL6 peptide inhibition RI-BPI in human pre-BCR+ ALL cells. (**A**) 697 cells were transduced with BCL6 shRNA (pCL6-TRRIP-BCL6-shRNA).Transduction efficiency with Puromycin selection and Doxycycline induction were verified by flow cytometry based on RFP. (**B**) BCL6 shRNA knockdown before and after Puro selection and Dox induction (0.5 μg/mL, 72 hr) was validated by Western blot with β-actin as a loading control. (**C**) 10,000 doxycycline-treated or untreated 697 cells were plated in semi-solid methylcellulose agar and colonies were counted after 10 days. Y axis shows percent colony formation measured at day 10. Data represent means ± SEM (n=3). P values from t-test. (**D**) Human pre-BCR^{+} *TCF3-PBX1* ALL cells were exposed to 5 uM retro-inverso BCL6 peptide-inhibitor (RI-BPI) or vehicle for 24 hr followed by BRDU or (**E**) 48 hr followed by colony formation assays. 10,000 cells were plated in semi-solid methylcellulose agar and colonies were counted after 10 days. (**F**) Human *TCF3-PBX1* ALL cells (ICN12, 697, RCH-ACV and Kasumi2) were treated for 72 hr with vehicle control, Vincristine (1 nM), RI-BPI (5 uM), or combination of Vincristine (1 nM) and RI-BPI (5 uM), followed by flow cytometry for Annexin V and 7-AAD staining. Bar plot data represents means of percentage of alive and dead cells. Data represent means ± SEM (n=3). All p values were calculated by t-test.

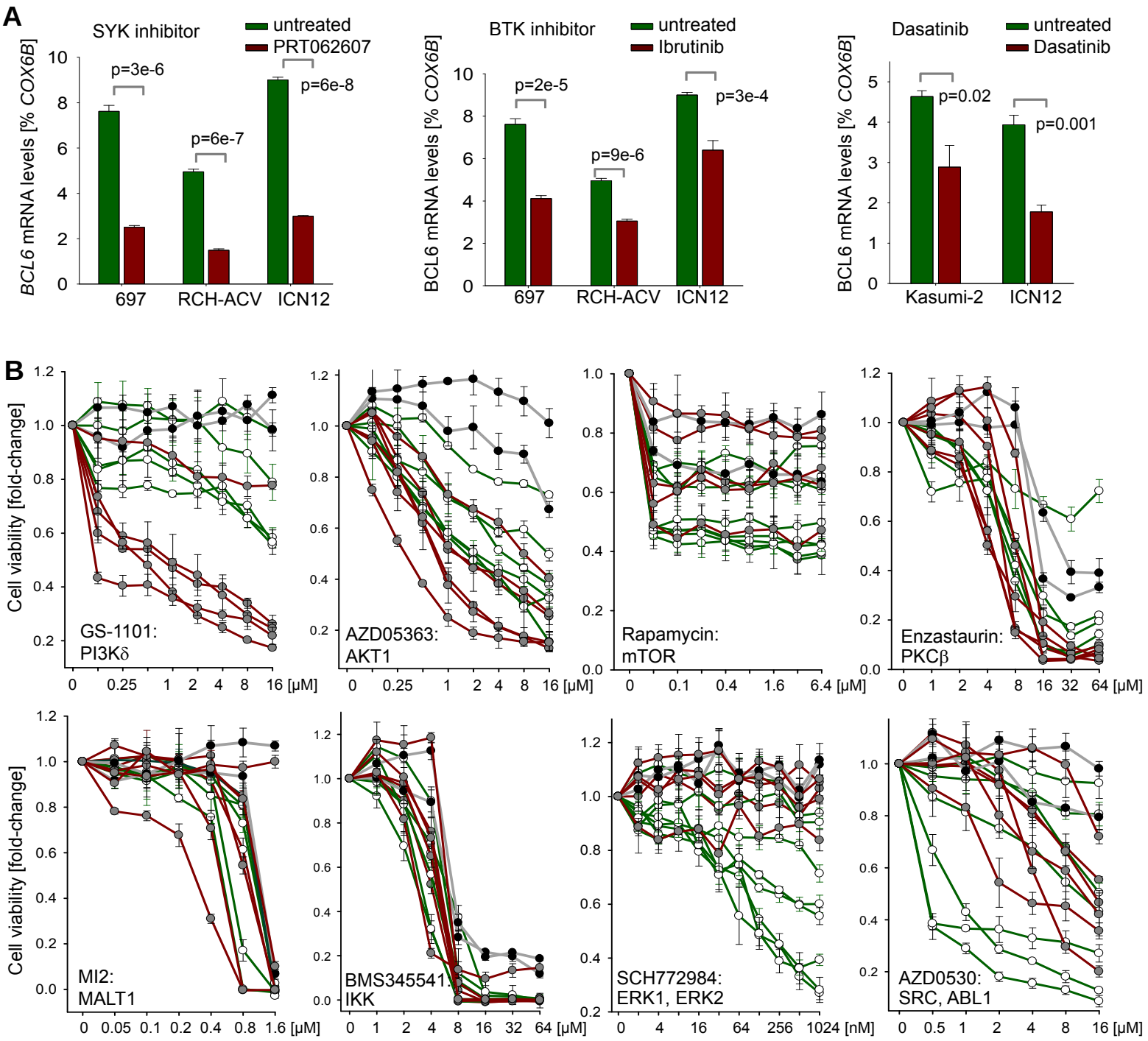
A
SYK inhibitor
untreated
PRT062607
BCL6 mRNA levels [% COX6B]
p=3e-6
p=6e-7
p=6e-8
697
RCH-ACV
ICN12
BTK inhibitor
untreated
Ibrutinib
BCL6 mRNA levels [% COX6B]
p=2e-5
p=9e-6
p=3e-4
697
RCH-ACV
ICN12
Dasatinib
untreated
Dasatinib
BCL6 mRNA levels [% COX6B]
p=0.02
p=0.001
Kasumi-2
ICN12
B
Cell viability [fold-change]
GS-1101:
PI3Kδ
AZD05363:
AKT1
Rapamycin:
mTOR
Enzastaurin:
PKCβ
MI2:
MALT1
BMS345541:
IKK
SCH772984:
ERK1, ERK2
AZD0530:
SRC, ABL1
Pre-BCR+: ICN12, 697, RCH-ACV, Kasumi-2, HPB-null, Nalm6
Pre-BCR-: TOM1, BV173, PDX2, BLQ5,LAX2, SEM, BEL1,REH
Burkitt's lymphoma: MN60, MHH-preB

Figure S6. Related to Figure 7. Validation of BCL6-pre-BCR signaling as therapeutic target in pre-BCR^{+} ALL. (**A**) *BCL6* mRNA expression was measured by qTR-PCR in presence or absence of SYK inhibitor PRT062607 (10 μM 24 hr), BTK inhibitor PCI-32765 (10 μM 24 hr), or Dasatinib (25 nM 24 hr) in *TCF3-PBX1* ALL cells. Y axis shows the *BCL6* mRNA expression normalized to *COX6B*. Data represent means ± SEM (n=3). P values from t-test. (**B**) pre-BCR^{+} ALL cells (n=6, ICN12, 697, RCH-ACV, Kasumi-2, HPB-null and Nalm6), pre-BCR^{-} ALL cells (n=8, TOM1, BV173, BLQ5, LAX2, PDX2, SEM, BEL1 and REH) and mature B cell lymphoma cells (n=2, MN60 and MHH-preB) were treated with inhibitors of pre-BCR downstream signaling GS-1101 (PI3Kδ), AZD05363 (AKT1), Rapamycin (mTOR), AZD0530 (SRC, ABL1), SCH772984 (ERK1, ERK2), Enzastaurin (PKCβ), MI2 (MALT1), BMS345541 (IKK, NF-kB) at various concentrations and cell viability was measured by CCK-8 at different dose levels. Data represent means ± SD (n=3).

SUPPLEMENTAL EXPERIMENTAL PROCEDURES

Primary Human Samples and Human Cell Lines

Primary ALL cases were obtained with the approval of the Institutional Review Boards of the University of California San Francisco (UCSF) and Oregon Health and Science University (OHSU). Primary human ALL samples were cultured on OP9 stroma in Minimum Essential Medium (MEMα, Life Technologies) with GlutaMAX containing 20% FBS, 100 IU ml^{-1} penicillin, 100 µg ml^{-1} streptomycin and 1mM sodium pyruvate at 37°C in a humidified incubator with 5% CO_2. The human cell lines were purchased from DSMZ (Braunschweig, Germany). See Table S1-S3.

Extraction of Bone Marrow Cells from Mice

Bone marrow cells were extracted from 4-6 week old *Bcl6*$^{fl/fl}$ mice. Bone marrow cells were obtained by flushing cavities of femur and tibia with PBS. After filtration through a 40 µm filter and depletion of erythrocytes using a lysis buffer (BD PharmLyse, BD Biosciences), washed cells were either frozen for storage or subjected to further experiments. All mouse experiments were subject to institutional approval by the University of California San Francisco Institutional Animal Care and Use Committee. The tables below showed mouse models used in this study and *Bcl6*$^{fl/fl}$ genotyping primers.

Overview of genetic mouse models

Mouse strain	Source	Purpose
[a] *Stat5*$^{fl/fl}$	Lothar Hennighausen, NIDDK	Cre mediated deletion of *Stat5a/b*
[b] *Blnk*$^{-/-}$	Hassan Jumaa, Max-Planck-Institute Freiburg	Reconstitution of Blnk expression
Ighm$^{-/-}$	Jackson Laboratories	Reconstitution of µ-chain expression
[c] *Rag2*$^{-/-}$ tTA/µ-tg	Hans-Martin Jäck, Universität Erlangen	Inducible activation of pre-B cell receptor signaling
Bcl6$^{fl/fl}$	Markus Muschen (UCSF), Ari Melnick (Weill Cornell), Hilde B. Ye (Albert Einstein)	Cre mediated deletion of *Bcl6*
[d] *BCR-ABL1*-tg	Nora Heisterkamp, CHLA	*BCR-ABL1* transgenic mouse model for Ph$^+$ pre-B ALL
[e] *TCF3-PBX1*-tg	Janetta J. Bijl, Hôpital Maisonneuve-Rosemont, Montreal, Canada	*TCF3-PBX1*-tg mouse model for t(1;19)(q23; p13.3) pre-B ALL
[f] *LSL-MLL-AF4*	Scott Armstrong, MSKCC	loxP-Stop-loxP *MLL-AF4* mouse model for t(4;11)(q21;q23) pre-B ALL
[g] *CD3ε*$^{-/-}$	Janetta J. Bijl, Hôpital Maisonneuve-Rosemont, Montreal, Canada	CD3ε mutant mouse
NOD/SCID	Jackson Laboratories	Xenograft recipient mice
NOD/SCID/IL-2rγ^{null}	Jackson Laboratories	Xenograft recipient mice

a, *Stat5*$^{fl/fl}$: Liu et al., *Genes Dev*. 1997; 11:179–186.
b, *Blnk*$^{-/-}$: Jumaa et al. *Immunity* 1999; 11: 547-54.
c, *Rag2*$^{-/-}$ tTA/µ-chain-tg: Hess et la. *PNAS* 2001*;* 98(4):1745-50.
d, *BCR-ABL1-tg* : Heisterkamp et al. *Nature* 1990; 344:251-3.
e, *TCF3-PBX1-tg* : Bijl et al. *Genes Dev*. 2005;19(2):224-33..
f, *MLL-AF4-tg* : Krivtsov et al. *Cancer Cell*. 2008;14(5):355-68.
g, Malissen, et al. *EMBO J* 1995; 14: 4641–4653.

Genotyping PCR primers for BCL6$^{fl/fl}$ mouse cells

Cre-mediated Bcl6 deletion, product size for *Bcl6* WT: 417 bp; Flox allele: 533 bp; Cre deleted allele: 345 bp

Bcl6-Cre_F	5'-CCTTGAAGGAGTTTTGCATGTGGG-3'
Bcl6-Cre_R	5'-GGTTTAAGTGCAGGGGCCATTTC-3'
Bcl6_R	5'-CCTTGAAGCGCATGAACTCCTTG-3'

Bcl6 targeted mutation, product size for *Bcl6* WT: 193 bp; Flox allele: 1.4 kbp

Bcl6_F	5'-CACAAACGTCATAGTCTCTCCAACCTC-3'
Bcl6_R	5'-CTGAATGCGTGGATGCCGAGAG-3'

Single-cell PCR and Sequence Analysis of V_H-DJ_H Gene Rearrangements

Normal human pro-B cells ($CD19^+CD34^+VpreB^-$), pre-B cells ($CD19^+CD34^-VpreB^+$) and immature B cells ($CD19^+CD10^+CD20^+$) were sorted from human bone marrow from four healthy donors (Cambrex, Verviers, Belgium) by flow cytometry using antibodies (BD Biosciences) and a FACSVantage SE cell sorter (BD Biosciences). Single cells from each population were sorted into individual PCR reaction tubes (containing 20 µL 1X PCR buffer) for single-cell PCR analysis of Ig V_H-DJ_H gene rearrangements, as previously described (Trageser et al., 2009). In addition, 148 primary ALL samples were analyzed with Ig V_H-DJ_H gene rearrangements, including 7 *MLL-AF4*, 57 *BCR-ABL1*, 13 *ETV6-RUNX1*, 30 Hyperdiploid, 33 not otherwise specified, and 8 *TCF3-PBX1* ALL. The primary ALL samples or the cDNA of primary ALL samples were provided from the Departments of Hematology and Oncology, University Hospital Benjamin Franklin, Berlin, Germany (W.K. Hoffman), the University of Bologna, Bologna, Italy (G. Martinelli), and the Department of Medical Biosciences, Umea University, Umea, Sweden (A. Li) and the USC Norris Comprehensive Cancer Center in compliance with Institutional Review Board regulations (approval from the Ethik-Kommission of the Charité, Campus Benjamin Franklin and the Internal Review Board of the University of Southern California Health Sciences Campus). PCR primer sets are listed below.

Single cell PCR for IGHM gene arrangement for human cells

V_H1	5'-CAGTCTGGGGCTGAGGTGAAGA-3'
V_H2	5'-GTCCTRCGCTGGTGAAACCCACACA-3'
V_H3	5'-GGGGTCCCTGAGACTCTCCTGTGCAG-3'
V_H4	5'-GACCCTGTCCCTCACCTGCRCTGTC-3'
V_H5	5'-AAAAAGCCCGGGGAGTCTCTGARGA-3'
V_H6	5'-ACCTGTGCCATCTCCGGGGACAGTG-3'
3'J_H1.2.4.5	5'-ACCTGAGGAGACGGTGACCAGGGT-3'
3'J_H3	5'-ACCTGAAGAGACGGTGACCATTGT-3'
3'J_H6	5'-ACCTGAGGAGACGGTGACCGTGGT-3'
5'-J_H1.4.5	5'-GACGGTGACCAGGGTKCCCTGGCC-3'
5'-J_H2	5'-GACAGTGACCAGGGTGCCACGGCC-3'
5'-J_H3	5'-GACGGTGACCATTGTCCCTTGGCC-3'
5'-J_H6	5'-GACGGTGACCGTGGTCCCTTKGCC-3'

Measurement of Ca^{2+} Release in Response to pre–BCR Engagement

Human B- ALL cell lines or patient samples were treated with antibodies specific for the μ chain of human (antibody purchased from Jackson ImmunoResearch Laboratories; Cat. No: 109-006-129, AffiniPure F(ab')2 Fragment Goat Anti-Human IgM, Fc(5mu) Fragment Specific). Ca^{2+} release from cytoplasmic stores in response to preB cell receptor engagement was measured by loading of the cells with the lipophilic Fluo-4 dye (Invitrogen, Carlsbad, CA).

Flow Cytometry

Human and mouse samples were stained with FACS antibodies listed in the tables below according to manufacturer's instructions using FC Block as well as respective isotype controls. For apoptosis analyses, Annexin V, propidium iodide and 7-AAD were used (BD Biosciences).

Flow cytometry antibodies for human cells

Antigen	Clone ID	Manufacturer
CD19	HIB19 (human)	BD Biosciences
VpreB	HSL96 (human)	BD Biosciences
IGLL1 (λ5)	HSL11 (human)	BD Biosciences
μHC (intracellular)	G20-127 (human)	BD Biosciences

Flow cytometry antibodies for mouse cells

Antigen	Clone ID	Manufacturer
CD19	1D3 (mouse)	BD Biosciences
CD25	7D4 (mouse)	BD Biosciences
CD8	53-6.7 (mouse)	BD Biosciences
CD43	S7 (mouse)	BD Biosciences
CD79B	HM79-12 (mouse)	BD Biosciences
IgM	R6-60.2 (mouse)	BD Biosciences
μHC (intracellular)	II/41 (mouse)	BD Biosciences
Bcl6 (intracellular)	K112-91 (mouse)	BD Biosciences
Blimp1 (intracellular)	5E7 (mouse)	BD Biosciences

Western Blotting

Cells were lysed in CelLytic buffer (Sigma) supplemented with 1% protease inhibitor cocktail (Pierce), 1% Phosphatase inhibitor cocktail (Calbiochem Millipore) and 1mM PMSF. Protein samples were loaded on NuPAGE (Invitrogen) 4-12% Bis-Tris gradient gels and transferred on Nitrocellulose membranes (Invitrogen). For the detection of mouse and human proteins by Western blot, primary antibodies were used together with the WesternBreeze immunodetection system (Invitrogen). The antibodies used for Western blotting are listed in the table below.

Western blot antibodies

Antigen	Clone ID	Manufacturer
BCL6	sc-7388	Santa Cruz Biotech.
STAT5	4459 (Figure 4D, left panel), 9363 (the rest)	Cell Signaling
P-STAT5^{Y694}	9351	Cell Signaling
BLK	3262	Cell Signaling
P-BLK^{Y388}	ab151726	Abcam
BTK	3532	Cell Signaling
P-BTK^{Y223}	5082	Cell Signaling
SYK	13198	Cell Signaling
P-SYK^{Y352}	2717	Cell Signaling
LYN	2796	Cell Signaling
P-SRC^{Y416}	6943	Cell Signaling
PLCγ2	3872	Cell Signaling
P-PLCγ2^{Y1217}	3871	Cell Signaling
ACTB	ab8227	Abcam

Colony-Forming Assay

10,000 *TCF3-PBX1* ALL cells were treated either with 5 *μ*M retro-inverso BCL6 peptide-inhibitor (RI-BPI) or vehicle control for 2 hr and then plated in semisolid agar (containing 5 *μ*M RI-BPI) for the methylcellulose colony-forming assays. Colonies were counted about 10 days after plating.

Cell-Cycle Analysis

The BrdU flow cytometry kit for cell-cycle analysis (BD Biosciences) was used according to manufacturer's instructions. BrdU incorporation (APC-labelled anti-BrdU antibodies) was measured with DNA content (7-ADD) in fixed and permeabilized cells. The analysis was gated on viable cells that were identified based on scatter morphology.

Cell Proliferation and Viability Assay

One hundred thousand human leukemia cells using cell lines or primary samples were seeded in a volume of 100 µL B cell medium (as described in "Primary human samples and human cell lines") per well on Optilux 96-well plate (BD Biosciences, San Jose, CA). SYK inhibitor (PRT062607), BTK inhibitor (PCI-32765 or Ibrutinib), or Dasatinib were diluted in medium and added at the indicated concentration in a total culture volume of 150 uL. After culturing for 72 hr, cell proliferation and viability was measured by Cell Counting Kit 8 (CCK-8; Dojindo Inc. Rockville, MD) according to the manufacturer's instructions. The fluorescence was read at 450 nm. Fold changes were calculated using baseline values of untreated cells as a reference (set to 100%).

Retroviral and Lentiviral Transduction

Transfections of the MSCV-based retroviral constructs were performed using Lipofectamine 2000 (Invitrogen, Carlsbad, CA) with Opti-MEM media (Invitrogen). Retroviral supernatant was produced by co-transfecting 293FT cells with the plasmids pHIT60 (gag-pol) and pHIT123 (ecotropic env; kindly provided by Donald B Kohn, UCLA). Cultivation was performed in high glucose Dulbecco's modified Eagle's medium (DMEM, Invitrogen) with GlutaMAX containing 10% fetal bovine serum, 100 IU/mL penicillin, 100 µg/mL streptomycin, 25 mM HEPES, 1 mM sodium pyruvate and 0.1 mM non-essential amino acids. Regular media were replaced after 16 hr by growth media containing 10 mM sodium butyrate. After 8 hr incubation, the media was changed back to regular growth media. 24 hr later, the virus supernatant were harvested, filtered through a 0.45 µm filter and loaded by centrifugation (2000 x g, 90 min at 32°C) two times on 50 ug/mL RetroNectin (Takara, Madison, WI) coated non-tissue 6-well plates. 1-2 x 10^6 pre-B cells were transduced per well by centrifugation at 600 x g for 30 min and maintained for 72 hr at 37°C with 5% CO2 before transferring into culture flasks.

Human BCL6 shRNA were ordered from Invitrogen (Carlsbad, CA; BCL6 shRNA sequence: 5'-GCTGTTGACAGTGAGCGCACAGACCAGTTGAAATGCAACTAGTGAAGCCACAGATGTAGTTGCATT TCAACTGGTCTGTATGCCTACTGCCTCGGA-3') and cloned into a "pCL6-TRRIP" lentiviral vector (Open Biosystems, Pittsburgh, PA) as described in (Park et al., 2011). Human *TCF3-PBX1* ALL cells were transduced with pCL6-TRRIP-BCL6-shRNA. Puromycin selection of transduced cells (sorting by FACS) was done before doxycycline induction (0.5 µg/mL) 72 hr before quantification of BCL6 knock-down.

Retroviral vector systems used

Construct	Overexpression of	Purpose
Constitutive expression		
MSCV IRES-GFP	GFP	Empty vector control
MSCV IRES-CD8	CD8	Empty vector control
MSCV IRES-Neo	Neomycin resistance	Empty vector control
MSCV Cre-IRES-GFP	Cre; GFP	Activation of Cre
MSCV BCR-ABL1-Neo	BCR-ABL1	Leukemic transformation (*BCR-ABL1* ALL)
MSCV TCF3-PBX1-Neo	TCF3-PBX1	Leukemic transformation (*TCF3-PBX1* ALL)
MSCV MLL-ENL-Neo	MLL-ENL	Leukemic transformation (*MLL-ENL* ALL)
MSCV BLNK-IRES-GFP	BLNK	Reconstitution of BLNK
MSCV IGHµ-IRES-CD8	IGHM (µ-chain)	Reconstitution of µ-chain
MSCV BCL6-IRES-GFP	BCL6	Reconstitution of BCL6
pCL6-LUC-Blast	Luciferase	Detection of human leukemic cells *in vivo*
Inducible expression		
MSCV - ER^{T2}-IRES-Puro	Puromycin resistance	Empty vector control
MSCV - ER^{T2}-IRES-GFP	GFP	Empty vector control
MSCV - Cre-ER^{T2}-IRES-Puro	Cre; Puromycin resistance	Inducible activation of Cre
MSCV - Cre-ER^{T2}-IRES-GFP	Cre; GFP	Inducible activation of Cre

MSCV-TCF3-PBX1-ER-Neo	TCF3-PBX1	Inducible expression of TCF3-PBX1
MSCV DN-BCL6-ERT2-GFP	DN-BCL6	Inducible expression of DN-BCL6

Quantitative Real-time PCR (qRT-PCR)

Total RNA from cells was extracted using RNeasy isolation kit from Qiagen (Valencia, CA) or NucleoSPIN RNA from Macherey-Nagel (Bethlehem, PA). cDNA was generated using a poly(dT) oligonucleotide and the SuperScript III Reverse Transcriptase (Invitrogen, Carlsbad, CA). Quantitative real-time PCR was performed with FAST SYBR® Green Master Mix (Applied Biosystems, Foster City, CA) and the Vii7 real-time PCR system (Applied Biosystems, Foster City, CA) according to standard PCR conditions. Primers for quantitative RT-PCR are listed in the table below.

Quantitative RT-PCR primers for human cells

BCL6_F	5'-TGAGAAGCCCTATCCCTGTG-3'
BCL6_R	5'-TGTGACGGAAATGCAGGTTA-3'
PRDM1_F	5'-GAATACGGTGTCCCCTGTGG-3'
PRDM1_R	5'-GGGTAGGAGCCCAAACCTTC-3'
GAPDH_F	5'-TTAGCACCCCTGGCCAAGG-3'
GAPDH_R	5'-CTTACTCCTTGGAGGCCATG-3'
COX6b_F	5'-AACTACAAGACCGCCCCTTT-3'
COX6b_R	5'- GCAGCCAGTTCAGATCTTCC -3'

Immunohistochemistry

The BCL6 immunohistochemistry was performed at UCSF Immunohistochemistry and Molecular Pathology Core Facility as described in (Deucher A et al., 2015). The cytoplasmic μHC immunohistochemistry was performed at USC clinical laboratory. Routinely processed paraffin-embedded tissue sections were used for the immunhistochemical studies. The sections were cut at 4 um and mounted onto slides. For the BCL6 studies, a Burkitt lymphoma bone marrow sample acted as a positive control and a chronic myeloid leukemia sample acted as a negative control. Immunohistochemical analysis was performed using a prediluted BCL6 antibody (mouse, monoclonal, clone GI191E/A8, Cell Marque, Rocklin, CA). Briefly, a DAKO Target Retrevial Solution (DAKO, Carpinteria, CA) at pH 6.0 was applied to the slides; they were then put into the pressure cooker. Following washing, blocking was performed using 3% H_2O_2, and the slides were then loaded onto an Immunostainer (Life Technologies, Carlsbad, CA). The secondary antibody was the EnVision+ system (DAKO, Carpinteria, CA). The slides were counterstained using hematoxylin and blue and then dehydrated in graded ethanols and covered with a coverslip. Expression of BCL6 in B-cell lymphoblastic leukemia cells was evaluated independently by a pathologist with the sample information blinded. BCL6 positive was called based on at least 50% of the cells are stained positive, weak positive when >20% of the cells are positively stained, and negative when <20% of the cells are stained BCL6 positive. The

double staining of BCL6 (nuclear, brown; Clone ID: PG-B6p; DAKO, Carpinteria, CA USA) and μHC (cytoplasmic/membrane, red; Clone ID: 8H6; Novocastra, Leica Biosystems, Buffalo Grove, IL USA) was performed at USC clinical laboratory.

Fluorescence in Situ Hybridization (FISH)

FISH was performed using Abbott LSI TCF3-PBX1 Dual Color Dual Fusion Translocation Probe (Abbott Molecular, Abbott Park, IL) following the manufacturer's protocol. The cells were counterstained with DAPI I (Abbott Molecular, Abbott Park, IL). FISH results were analyzed and documented using CytoVision System (Leica Microsystems, Buffalo Grove, IL).

Tyrosine Kinase Inhibitors and BCL6 Inhibitors

The tyrosine kinase inhibitors were purchased from the following catalog numbers and companies: PRT062607 (SYK): S8032, SelleckChem; Ibrutinib (BTK): S2680, SelleckChem; Dasatinib (SRC): D-3307, LC Labs; GS-1101 (PI3Kδ): CT-CAL101, ChemieTek; AZD05363 (AKT1): CT-A5363, ChemieTek; Rapamycin (mTOR): S1039, SelleckChem; AZD0530 (SRC/ABL1): S1006, SelleckChem; SCH772984 (ERK1, ERK2): S7101, SelleckChem; Enzastaurin (PKCβ): S1055, SelleckChem; MI2 (MALT1): 500491, EMD Millipore; BMS345541 (IKK, NF-κB): HY-10518, MedChem Express. Integrating experimentally measured sensitivities to individual inhibitors with their known inhibitory profile based on biochemical IC_{50} values for individual kinase targets, a kinase dendrogram of specific vulnerabilities of pre-BCR^{+} and pre-BCR^{-} ALL was plotted using TREESpots software (KINOMEscan®, http://www.discoverx.com/services/drug-discovery-development-services/treespot-data-analysis). The peptidomimetic BCL6 inhibitor RI-BPI (Cerchietti et al., 2009) was synthesized by Biosynthesis, Inc. (Lewisville, TX; amino acids sequence: GRRRQRRKKRGGRGIEHISRGGDIMGEWGNEIFGAIAGFLG; purity >95% by high-performance liquid chromatography-mass spectrometry). RI-BPI was stored at -20ºC until reconstituted with sterile, distilled, degassed water immediately before use.

***In Vitro* Drug Sensitivity**

In vitro drug sensitivity assays were performed as previously described (Tyner et al., 2013). Briefly, mononuclear cells were separated by Ficoll gradient, and then underwent erythrocyte lysis with Ammonium-Chloride-Potassium (ACK) lysing buffer from Invitrogen (Grand Island, NY). Cells were then incubated in increasing concentrations of drug for three days at 37˚C, 5% CO2 in R20 [RPMI-1640 medium supplemented with 20% FBS, L-glutamine, penicillin/streptomycin, and fungizone supplemented with 10^{-4} M 2-mercaptoethanol], then subjected to MTS as a marker for relative cell viability. IC_{50} values were calculated using second-degree polynomial regression curves fit through 5 data points (average of

no drug wells and 4 serial dilution points), as previously described in (Tyner et al., 2013). Where an IC_{50} was not achieved for a given drug, an IC_{50} value equal to the highest drug concentration used was arbitrarily assigned. All curves were manually inspected. For a given sample, its sensitivity to a drug was defined as the percentage of the drug IC_{50} value in this sample to the median IC_{50} value which was computed from over 400 primary leukemia samples interrogated by this assay at Oregon Health & Science University (Portland, OR; Tyner et al., 2013).

***In Vivo* Leukemia Cell Transplantation and Treatment (07-112, 11-064, 09-565)**

All animal studies were conducted with approval from OHSU's Institutional Animal Care and Use Committee. Veterinary care was provided through the OHSU Department of Comparative Medicine. NOD/SCID/IL-2rγ^{null} (NSG) mice were sub-lethally irradiated with 200 centigray at age 6 wk, anesthetized with isofluorane and injected 24 hr later via tail vein with 0.5-3 million cells from frozen patient samples. Mice were then placed on ciprofloxacin (0.25 mg/ml) containing water for 4 wk during recovery. They were then maintained on acidified water of 1mM HCl. Peripheral blood was monitored weekly starting on week 3 by flow cytometry for human engraftment using antibodies against human CD19 and CD45 (hCD19-APC, hCD45-FITC) versus murine CD45 (mCD45-PerCP-Cy5.5). Flow cytometric data was analyzed using FACS/AriaIII. When the mice were determined to be engrafted with >10% human chimerism in peripheral blood, the animals were euthanized and secondary xenografts were established from leukemic cells harvested from the spleen and used for treatment. Cohorts of NSG mice were again injected as described above. One week after tail vein injection of leukemic cells, the mice were divided into two groups and treated by oral gavage with dasatinib at 50 mg/kg/dose daily or citrate control for 5 days/week as previously described (Bicocca et al., 2012; Kolb et al., 2008). Treatment continued until the day of sacrifice (4-20 wk). Peripheral blood was again monitored weekly starting on week 3 by flow cytometry for human engraftment. When the mice were determined to be engrafted, or became too ill according to standard parameters set by the Institutional Animal Care and Use Committee protocol, they were euthanized via general anesthesia and cervical dislocation. Bone marrow and spleen were harvested at the time sacrifice.

***In Vivo* Leukemia Cell Transplantation and Treatment (ICN12)**

All mouse experiments were subject to institutional approval by the University of California San Francisco Institutional Animal Care and Use Committee. 1 x 10^6 cells from a bone marrow biopsy of a patient with *TCF3-PBX1* pre-BCR$^+$ ALL (ICN12) were inoculated via intravenous (I.V.) injection into sublethally irradiated (250 cGy) adult female NOD/SCID mice (n=28). After injection of leukemia cells the mice were randomly separated into four groups. The first group was treated by oral gavage with

Dasatinib (40 mg/kg); the second group was treated by oral gavage with Ibrutinib (75 mg/kg); the third group was treated with PRT062607 (100 mg/kg); the fourth group was treated with vehicle and used as controls. Mouse survival was monitored. When the mice became terminally ill because of overt leukemia, they were sacrificed and leukemia cells were harvested from bone marrow and spleen. Leukemic infiltration was confirmed by flow cytometry. Pictures were taken using a digital camera (Olympus DP72) attached to a light microscope (Axioskop, Carl Zeiss) with 34 and 320 Plan Neofluar objectives (Carl Zeiss).

Chromatin Immunoprecipitation (ChIP) and QChIP

697 cells were fixed with 1% formaldehyde, lysed and sonicated to generate fragments less than 500 bp. ICN12 cells were treated similarly except they were initially fixed first with 2 mM Di (N-succinimidyl) glutarate before 1% formaldehyde fixation. Antibodies used are listed in the table below. Sonicated lysates were incubated with antibodies overnight and after increasing stringency washes immunocomplexes were recovered and DNA was isolated. The ChIP protocol was performed as in Geng et al.(Geng et al., 2012). A fraction (0.2 ng) of the input and the ChIPed DNA were used as templates in QPCR reactions using SYBR Green^{TM} and a 7300 ABI qRT-QPCR machine (Applied Biosystems, CA). The QChIP results were quantified and shown as fold enrichment relative to inputs. A stable 697 line with inducible expression of TCF3-PBX1-hf (HA-FLAG tag) was established by co-infection with a human EF1a promoter-driven regulatory rtTA3 and a tetracycline response element promoter-driven TCF3-PBX1-hf expressing lentiviral constructs (kind gifts of Dr. Robert Roeder, Rockefeller University). Positive clones were isolated by standard serial dilution method with puromycin selection (Puromycin resistance gene is encoded by rtTA3 lentiviral construct). The QChIP antibodies and primer sequences are provided in the table below.

Antibodies used for ChIP-seq and QChIP for human cells

Antibody	Clone ID	Manufacturer
$TCF3^{N}$	12258	Cell Signaling
$PBX1/2/3^{C}$	sc-888	Santa Cruz
p300	sc-585	Santa Cruz
Anti-HA-tag	ab9110	Abcam
BCL6	4242	Cell Signaling
IgG	2729	Cell Signaling

Quantitative ChIP primers for TCF3-PBX1 fusion protein binding in 697 cells

Target promoter	Forward primer (5'→ 3')	Reverse primer (5'→ 3')
IGLL1 (λ5)	CACAGCAGGGCAGTTGGCAGATG	CGCTGGCAGCAGCTGTCCCATTG
VpreB1	ACCCAAAGGCCTCCAGGGCA	ACCGGAACAGTGTCGGGGCA
VpreB3	CACAGACTCCAAGGGGTAGG	TGGTAGCCTGACCTTCCTGT

CD79A (Igα)	CAGGGAAGGGACAAGGTTTG	ACCTGTGGTGGCCACAATTC
CD79B (Igβ)	CGAGGCTCCTTGGAGGAAAA	GGTCCCAATTTGCATGGCAG
IgH Eμ	TCACTTCTGGTTGTGAAGAGGTGG	GTTTCGGTCAGCCTCGCCTTATTT
BCL6	GGAAATCCTTACGGCTTGGCAG	GGGCTGAGGGTCTCCATCATAGG
NCAPD2	ATGGTTGCCACTGGGGATCT	TGCCAAAGCCTAGGGGAAGA

Quantitative ChIP primers for TCF3-PBX1 fusion protein binding in ICN12 and RCH-ACV cells

Target promoter	**Forward primer (5'→ 3')**	**Reverse primer (5'→ 3')**
IGLL1 (λ5)	GTCAGGATCCAGGGCTCAAC	GTGGGAGGTCCCCAAACAAA
VpreB1	CCCATGCCTGAGTCACTCTAC	GAGCGGGTTGGGATGTTCT
VpreB3	GCCACCCTAGAGCCATAACC	ACTGGTAGCCTGACCTTCCT
CD79A (Igα)	GGGACTGCTGCAACTCAAAC	TGGCCACATACCCAGGTAGA
CD79B (Igβ)	GCCCTAGGGACCATTGTTTG	TCAGACTTTCCCAGCCTCAT
IgH Eμ	ACCACCTCTTCACAACCAGA	GGTCACCGCGAGAGTCTA
BCL6	CGTAGCAGTGGTAAAGTCCGAAGC	GCAGCAACAGCAATAATCACCTGG
Control	GGCTCCTGTAACCAACCACTACC	CCTCTGGGCTGGCTTCATTC

Quantitative ChIP primers for BCL6 binding in ICN12 cells

Target promoter	**Forward primer (5' → 3')**	**Reverse primer (5' → 3')**
BCL6	CGTAGCAGTGGTAAAGTCCGAAGC	GCAGCAACAGCAATAATCACCTGG
CDKN1B	GGTGATACCACAGGCTCAAGA	GTTGCCTGCAGATGTTTCCT
CDKN2C	GAACAAGGGTGGGTGAATGC	CCGCGGAAGGAAAGACATTC
EBF3	AGGCTCTTAGGGCTTGCATT	GCTCTCCACCAGGCAAGTT
IKZF2	CAGGCAGATGAGGGCTCAATA	TCCTTGACAGCATGCATGAC
IRF4	CCATCGCAGTGGAACTCAG	AGGGGAGAACAATCGTAACAAC
PRDM1	CAGTCCGAGGAAGGCTAACT	GGGTTCCATCGCTCTTGTACT
RB1	TTGCGGCGTTTCCTTAGAAC	AAGCCGACTAACACGCAAGA
COX6b	CTGTCCGACTGTGGTGTCTT	TCAACCTGCAGCTCAATGTG
Control	GGCTCCTGTAACCAACCACTACC	CCTCTGGGCTGGCTTCATTC

Genomic DNA-Fragment Library for ChIP Sequencing (ChIP-seq)

Genomic DNA-fragment libraries were prepared using the Illumina ChIP-seq Library preparation Kit following the manufacturer's instructions (Illumina, CA). Briefly 10ng of purified ChIP DNA was end repaired by conversion of overhangs into phosphorylated blunt ends with the use of T4 DNA polymerase and E. coli DNA polymerase I Klenow fragment. Illumina paired-end adapters were ligated to the ends of the DNA fragments. Ligation products were purified on a 2% agarose gel with a size selection of 200-300 bp. Fifteen PCR cycles were performed with Illumina genomic DNA primers that anneal to the ends of the adapters. The purified PCR-amplified fragment libraries were quantified with the use of the PicoGreen dsDNA Quantitation Assay with the Qubit Fluorometer (Invitrogen, CA). The size range of

libraries was validated on the Agilent Technologies 2100 Bioanalyzer with the High Sensitivity DNA Kit (Agilent, CA). After library preparation, the protocols for the Illumina Single-Read Cluster Generation Kit were used for cluster generation on the cBOT (Illumina). The targeted samples were diluted to 10 nmol and denatured with sodium hydroxide. Seven pico moles of each target-enriched sample and Phix control were loaded into separate lanes of the same flow cell, hybridized, and isothermally amplified. After linearization, blocking, and primer hybridization, sequencing was performed for 50 cycles on an Illumina HiSeq2000. Raw image data were converted into base calls via the Illumina pipeline CASAVA version 1.8 with default parameters. Rigorous quality control was performed with the use of data from reports generated by the Illumina pipeline.

ChIP-seq Data Analysis

All 50 bp-long reads were mapped to the reference human genome sequence, hg18, using BWA (Li and Durbin, 2009) aligner with the default parameters. Only reads mapping uniquely to the genome with not more than 2 mismatches were retained for further analysis. Clonal reads (i.e., reads mapping at the same genomic position and on the same strand) were collapsed into a single read. Peaks from ChIP-seq data were called using the ChIPseeqer program(Giannopoulou and Elemento, 2011) and annotated to gene promoters (+/- 2kb to TSS (transcription start site)) based on hg18 refseq genes downloaded from the UCSC Genome Browser. To estimate self-consistency and determine appropriate thresholds for binding sites peak calling, Irreproducibility Discovery Rate (IDR) analysis (Landt et al., 2012; Li et al., 2011) were performed for each of the mapped samples. Each mapped sample was randomly split into 2 pseudo-replicates with approximately equal number of reads. Peaks were then called from the two pseudo-replicates using ChIPseeqer-2.0 (Giannopoulou and Elemento, 2011). The output peak files were converted to the ENCODE narrowPeak format. Based on the ranking of peak p-values, IDR was calculated on the pseudo-replicates using the R scripts from https://sites.google.com/site/anshulkundaje/projects/idr.

Reverse Phase Protein Array (RPPA) Analysis

Proteomic profiling was performed using RPPA as described (Tibes et al., 2006). Briefly, samples were printed in 5 serial dilutions along with normalization and expression controls, with fractions from each patient clustered together. All samples were printed in replicate. Pearson correlation coefficients of duplicated samples within arrays had mean, median, and standard deviations of 0.84, 0.87, 0.09, respectively. Slides were probed with 133 validated primary antibodies, detecting total, phospho or cleaved proteins, and a secondary antibody to amplify the signal, and a stable dye is precipitated. The antibodies used in this study are listed in the table below. For the statistical analysis, relative protein

concentrations in $\log_2$ scale were estimated by fitting a common logistic response curve using all sample dilution series within an array. The algorithm was implemented in an R package, *SuperCurve.* A topographical normalization followed by a median polish procedure was used to account for within-array background staining and sample loading variations.

Antibodies used for reverse phase protein arrays

Antigen	Clone ID	Manufacturer
LYN	2732	Cell Signaling
AKT1	4691	Cell Signaling
AKT-pS473	9271	Cell Signaling
AKT-pT308	2965	Cell Signaling
ERK2	9108	Cell Signaling
ERK-pT202/Y204	9101	Cell Signaling
GAB2	3239	Cell Signaling
GAB2-pY452	3882	Cell Signaling
MEK-pS217/S221	9154	Cell Signaling
MEK	9125	Cell Signaling
mTOR	2983	Cell Signaling
MTOR-pS2448	2971	Cell Signaling
P38a	9228	Cell Signaling
p38	9212	Cell Signaling
P38a-pT180/Y182	9211	Cell Signaling
RPS6KB-S371	9205	Cell Signaling
PDK1	3062	Cell Signaling
PDK1-pS241	3061	Cell Signaling
PIK3CD	4255	Cell Signaling
PIK3R1	06-195	Millipore
PKCa	05-154	Millipore
PKCa-pS657	06-822	Millipore
PKCd-pS645	9371	Cell Signaling
PKCd-pS664	07-875	Millipore
PTEN	9552	Cell Signaling
PTEN-pS380	3539	Cell Signaling
RPS6-pS235/6	2211	Cell Signaling
RPS6-pS240/244	2215	Cell Signaling
SRC	05-184	Millipore
SRC-pY416	2101	Cell Signaling
SRC-pY527	2105	Cell Signaling
STAT5	9352	Cell Signaling
STAT5-pY694	9351	Cell Signaling

Patient Gene Expression Microarray and Outcome Data

Gene expression microarray data from three large cohorts of patients with pre-B ALL were downloaded from GSE5314 (Geng et al., 2012) (the Eastern Cooperative Oncology Group (ECOG) Clinical Trial E2993, n=191), GSE11877 (Harvey et al., 2010) (the Children's Oncology Group (COG) Clinical Trial P9906, n=207), St. Jude Research Hospital pediatric ALL (Ross et al., 2003) (n=132 ALL,

http://www.stjuderesearch.org/site/data/ALL3/), and normal pre-B samples (van Zelm et al., 2005, Trageser et al., 2009) (n=14, http://franklin.et.tudelft.nl/). Patient outcome data were obtained from the National Cancer Institute TARGET Data Matrix (http://target nci.nih.gov/dataMatrix/TARGET_DataMatrix.html) of the Children's Oncology Group (COG) Clinical Trial P9906 (Harvey et al., 2010; Hogan et al., 2011). The end point of the clinical data is overall survival (OS).

Pathway and Motif Analysis

The Ingenuity Pathway Analysis (IPA) software (Ingenuity Systems, Inc. Redwood City, CA) was also used to identify deregulated gene networks. The motif analysis was done with Cistrome DNA motif-finding analysis (Liu et al., 2011).

Statistical Analysis

The comparisons for the means between two groups were made by two-tailed t test or Wilcoxon's rank-sum test using R software (R Development Core Team 2009; http://www.r-project.org). The Kaplan-Meier method was used to estimate overall survival. Log-rank test was used to compare survival differences between patient groups. The R package 'survival' version 2.35-8 was used for the survival analysis. The level of significance was set at $p < 0.05$.

SUPPLEMENTAL REFERENCES

Bicocca, V. T., Chang, B. H., Masouleh, B. K., Muschen, M., Loriaux, M. M., Druker, B. J., and Tyner, J. W. (2012). Crosstalk between ROR1 and the Pre-B cell receptor promotes survival of t(1;19) acute lymphoblastic leukemia. Cancer Cell 22, 656-667.

Bijl J, Sauvageau M, Thompson A, Sauvageau G. (2005). High incidence of proviral integrations in the Hoxa locus in a new model of E2a–PBX1-induced B-cell leukemia. Genes Dev.19(2):224-33.

Deucher A, Yu J, Zhongxia Q, George T, and J., E. (2015). BCL6 expression correlates with the t (1;19) translocation (TCF3 (E2A)/PBX1) in B-cell lymphoblastic leukemia. American Journal of Clinical Pathology. In Press.

Giannopoulou, E. G., and Elemento, O. (2011). An integrated ChIP-seq analysis platform with customizable workflows. BMC Bioinformatics 12, 277.

Heisterkamp N, Jenster G, ten Hoeve J, Zovich D, Pattengale PK, Groffen J. (1990). Acute leukaemia in bcr/abl transgenic mice. Nature 344:251-3.

Hogan, L. E., Meyer, J. A., Yang, J., Wang, J., Wong, N., Yang, W., Condos, G., Hunger, S. P., Raetz, E., Saffery, R., et al. (2011). Integrated genomic analysis of relapsed childhood acute lymphoblastic leukemia reveals therapeutic strategies. Blood 118, 5218-5226.

Hess J, Werner A, Wirth T, Melchers F, Jäck HM, Winkler TH. (2001). Induction of pre-B cell proliferation after de novo synthesis of the pre-B cell receptor. Proc Natl Acad Sci U S A 98(4):1745-50.

Jumaa H, Wollscheid B, Mitterer M, Wienands J, Reth M, Nielsen PJ. (1999). Abnormal development and function of B lymphocytes in mice deficient for the signaling adaptor protein SLP-65. Immunity 11: 547-54.

Kolb, E. A., Gorlick, R., Houghton, P. J., Morton, C. L., Lock, R. B., Tajbakhsh, M., Reynolds, C. P., Maris, J. M., Keir, S. T., Billups, C. A., and Smith, M. A. (2008). Initial testing of dasatinib by the pediatric preclinical testing program. Pediatr Blood Cancer 50, 1198-1206.

Krivtsov AV, Feng Z, Lemieux ME, Faber J, Vempati S, Sinha AU, Xia X, Jesneck J, Bracken AP, Silverman LB, Kutok JL, Kung AL, Armstrong SA. (2008). H3K79 methylation profiles define murine and human MLL-AF4 leukemias. Cancer Cell 14(5):355-68.

Landt, S. G., Marinov, G. K., Kundaje, A., Kheradpour, P., Pauli, F., Batzoglou, S., Bernstein, B. E., Bickel, P., Brown, J. B., Cayting, P., et al. (2012). ChIP-seq guidelines and practices of the ENCODE and modENCODE consortia. Genome Res 22, 1813-1831.

Li, H., and Durbin, R. (2009). Fast and accurate short read alignment with Burrows-Wheeler transform. Bioinformatics 25, 1754-1760.

Li, Q., Brown, J. B., Huang, H., and Bickel, P. J. (2011). Measureing reporducibility of high-throughput experiments. The Annals of Applied Statistics 5, 1752–1779.

Liu, T., Ortiz, J. A., Taing, L., Meyer, C. A., Lee, B., Zhang, Y., Shin, H., Wong, S. S., Ma, J., Lei, Y., et al. (2011). Cistrome: an integrative platform for transcriptional regulation studies. Genome Biol 12, R83.

Liu X, Robinson GW, Wagner KU, Garrett L, Wynshaw-Boris A, Hennighausen L. (1997). Stat5a is mandatory for adult mammary gland development and lactogenesis. Genes Dev. 11:179–186.

Malissen, M., Gillet, A., Ardouin, L., Bouvier, G., Trucy, J.,Ferrier, P., Vivier, E., and Malissen, B. (1995). Altered T cell development in mice with a targeted mutation of the CD3-ε gene. EMBO J 14: 4641–4653.

Park, E., Gang, E. J., Hsieh, Y. T., Schaefer, P., Chae, S., Klemm, L., Huantes, S., Loh, M., Conway, E. M., Kang, E. S., et al. (2011). Targeting survivin overcomes drug resistance in acute lymphoblastic leukemia. Blood 118, 2191-2199.

van Zelm, M. C., van der Burg, M., de Ridder, D., Barendregt, B. H., de Haas, E. F., Reinders, M. J., Lankester, A. C., Revesz, T., Staal, F. J., and van Dongen, J. J. (2005). Ig gene rearrangement steps are initiated in early human precursor B cell subsets and correlate with specific transcription factor expression. J Immunol 175, 5912-5922.